A FINITE ELEMENT METHOD FOR NEMATIC LIQUID CRYSTALS WITH VARIABLE DEGREE OF ORIENTATION

RICARDO H. NOCHETTO[1], SHAWN W. WALKER[2], WUJUN ZHANG[3]

Abstract. We consider the simplest one-constant model, put forward by J. Ericksen, for nematic liquid crystals with variable degree of orientation. The equilibrium state is described by a director field $\mathbf{n}$ and its degree of orientation s, where the pair $(s, \mathbf{n})$ minimizes a sum of Frank-like energies and a double well potential. In particular, the Euler-Lagrange equations for the minimizer contain a degenerate elliptic equation for $\mathbf{n}$, which allows for line and plane defects to have finite energy.

We present a structure preserving discretization of the liquid crystal energy with piecewise linear finite elements that can handle the degenerate elliptic part without regularization, and show that it is consistent and stable. We prove Γ-convergence of discrete global minimizers to continuous ones as the mesh size goes to zero. We develop a quasi-gradient flow scheme for computing discrete equilibrium solutions and prove it has a strictly monotone energy decreasing property. We present simulations in two and three dimensions to illustrate the method's ability to handle non-trivial defects.

Key words. liquid crystals, finite element method, gamma-convergence, gradient flow, line defect, plane defect

AMS subject classifications. 65N30, 49M25, 35J70

1. Introduction.

Complex fluids are ubiquitous in nature and industrial processes and are critical for modern engineering systems [30, 39, 14]. An important difficulty in modeling and simulating complex fluids is their inherent microstructure. Manipulating the microstructure via external forces can enable control of the mechanical, chemical, optical, or thermal properties of the material. Liquid crystals [45, 24, 20, 3, 2, 12, 6, 31, 32, 4, 44] are a relatively simple example of a material with microstructure that may be immersed in a fluid with a free interface [51, 50].

Several numerical methods for liquid crystals have been proposed in [9, 28, 22, 33, 1] for harmonic mappings and liquid crystals with fixed degree of orientation, i.e. a unit vector field $\mathbf{n}(x)$ (called the director field) is used to represent the orientation of liquid crystal molecules. See [27, 34, 47] for methods that couple liquid crystals to Stokes flow. We also refer to the survey paper [5] for more numerical methods.

In this paper, we consider the one-constant model for liquid crystals with variable degree of orientation [25, 24, 45]. The state of the liquid crystal is described by a director field $\mathbf{n}(x)$ and a scalar function $s(x)$, $-1/2 < s < 1$, that represents the degree of alignment that molecules have with respect to $\mathbf{n}$. The equilibrium state is given by $(s, \mathbf{n})$ which minimizes the so-called one-constant Ericksen's energy (2.1).

Despite the simple form of the one-constant Ericksen's model, its minimizer may have non-trivial defects. If s is a non-vanishing constant, then the energy reduces to the Oseen-Frank energy whose minimizers are harmonic maps that may exhibit point defects (depending on boundary conditions) [13, 15, 19, 32, 31, 40]. If s is part of the minimization of (2.1), then s may vanish to allow for line (and plane) defects in dimension $d = 3$ [4, 44], and the resulting Euler-Lagrange equation for $\mathbf{n}$ is degenerate. However, in [32], it was shown that both s and $\mathbf{u} = s\mathbf{n}$ have strong limits, which enabled the study of regularity properties of minimizers and the size of defects. This inspired the study of dynamics [20] and corresponding numerics [7], which are most relevant to our paper. However, in both cases they regularize the model to avoid the degeneracy introduced by the s parameter.

[1]rhn@math.umd.edu, [2]walker@math.lsu.edu, [3]wujun@umd.edu.

We design a finite element method (FEM) *without* any regularization. We prove stability and convergence properties and explore equilibrium configurations of liquid crystals via quasi-gradient flows. Our method builds on [11, 8, 10] and consists of a structure preserving discretization of (2.1). Given a weakly acute mesh $\mathcal{T}_h$ with meshsize h (see Section 2.2), we use the subscript h to denote continuous piecewise linear functions defined over $\mathcal{T}_h$, e.g. $(s_h, \mathbf{n}_h)$ is a discrete approximation of $(s, \mathbf{n})$.

Our discretization of the energy is defined in (2.13) and requires that $\mathcal{T}_h$ be *weakly acute*. This discretization preserves the underlying structure and converges to the continuous energy in the sense of Γ-convergence [16] as h goes to zero. Next, we develop a quasi-gradient flow scheme for computing discrete equilibrium solutions. We prove that this scheme has a strictly monotone energy decreasing property. Finally, we carry out numerical experiments and show that our finite element method, and gradient flow, allows for computing minimizers that exhibit line and plane defects.

The paper is organized as follows. In Section 2, we describe the Ericksen model for liquid crystals with variable degree of orientation, as well as the details of our discretization. Section 3 shows the Γ-convergence of our numerical method. A quasi-gradient flow scheme is given in Section 4, where we also prove a strictly monotone energy decreasing property. Section 5 presents simulations in two and three dimensions that exhibit non-trivial defects in order to illustrate the method's capabilities.

2. Discretization of Ericksen's model.

We review the model [25] and relevant analysis results from the literature. We then develop our discretization strategy and show it is stable. In principle, the space dimension d can be arbitrary $d \geq 2$, but for some of the proofs we require $d = 2, 3$.

2.1. Ericksen's one constant model.

Let the director field $\mathbf{n} : \Omega \subset \mathbb{R}^d \to \mathbb{S}^{d-1}$ be a vector-valued function with unit length, and the degree of orientation $s : \Omega \subset \mathbb{R}^d \to [-\frac{1}{2}, 1]$ be a real valued function. The case $s = 1$ represents the state of perfect alignment in which all molecules are parallel to $\mathbf{n}$. Likewise, $s = -1/2$ represents the state of microscopic order in which all molecules are orthogonal to the orientation $\mathbf{n}$. When $s = 0$, the molecules do not lie along any preferred direction which represents the state of an isotropic distribution of molecules.

The equilibrium state of the liquid crystals is described by the pair $(s, \mathbf{n})$ minimizing a bulk-energy functional which in the simplest one-constant model reduces to

$$E[s, \mathbf{n}] := \underbrace{\int_\Omega \Big(\kappa |\nabla s|^2 + s^2 |\nabla \mathbf{n}|^2\Big) dx}_{=:E_1[s,\mathbf{n}]} + \underbrace{\int_\Omega \psi(s) dx}_{=:E_2[s]}, \tag{2.1}$$

with $\kappa > 0$ and double well potential ψ, which is a C^2 function defined on $-1/2 < s < 1$ that satisfies

1. $\lim_{s\to 1} \psi(s) = \lim_{s\to -1/2} \psi(s) = \infty$,
2. $\psi(0) > \psi(s^*) = \min_{s\in[-1/2,1]} \psi(s)$ for some $s^* \in (0, 1)$,
3. $\psi'(0) = 0$;

see [25]. By introducing an auxiliary variable $\mathbf{u} = s\mathbf{n}$, we rewrite the energy as

$$E_1[s, \mathbf{n}] = \widetilde{E}_1[s, \mathbf{u}] := \int_\Omega \Big((\kappa - 1)|\nabla s|^2 + |\nabla \mathbf{u}|^2\Big) dx, \tag{2.2}$$

which follows from the orthogonal splitting $\nabla \mathbf{u} = \mathbf{n} \otimes \nabla s + s\nabla \mathbf{n}$ due to the constraint $|\mathbf{n}| = 1$. Accordingly, we define the admissible class

$$\mathcal{A} := \{(s, \mathbf{n}) : \Omega \to [-1/2, 1] \times \mathbb{S}^{d-1},\ \text{where } s \in H^1(\Omega),\ \mathbf{u} = s\mathbf{n} \in H^1(\Omega)^d\}. \tag{2.3}$$

Moreover, we may also enforce boundary conditions on s and $\mathbf{n}$, possibly on different parts of the boundary. Let Γ_s ($\Gamma_{\mathbf{n}}$) be an open subset of $\partial\Omega$ where we will set Dirichlet boundary conditions for s ($\mathbf{n}$). Then we have the following restricted admissible class

$$\mathcal{A}(g,\mathbf{r}) := \left\{(s,\mathbf{n}) \in \mathcal{A} : s|_{\Gamma_s} = g, \quad \mathbf{n}|_{\Gamma_{\mathbf{n}}} = \mathbf{r}\right\}, \tag{2.4}$$

for some given smooth functions g and $\mathbf{r}$ such that $|\mathbf{r}| = 1$ and both g and $g\mathbf{r}$ are the traces of some $H^1(\Omega)$ functions.

Note that when the degree of orientation s equals a non-zero constant, the energy (2.1) effectively reduces to the Oseen-Frank energy $\int_\Omega |\nabla \mathbf{n}|^2$. The introduction of the degree of orientation relaxes the energy of defects. In fact, with finite energy $E[s,\mathbf{n}]$, defects (i.e. discontinuities in $\mathbf{n}$) may still occur in the singular set

$$\mathcal{S} := \{x \in \Omega,\ s(x) = 0\}. \tag{2.5}$$

The existence of such a minimizer in the admissible class subject to Dirichlet boundary conditions is shown in [32, 2]. It is worth mentioning that the constant κ in $E[s,\mathbf{n}]$ (2.1) plays a significant role in the occurrence of the defects. Roughly speaking, if κ is large, then $\int_\Omega \kappa|\nabla s|^2 dx$ dominates the energy and s is close to a constant. In this case, defects with finite energy are less likely to occur. But if κ is small, then $\int_\Omega s^2|\nabla \mathbf{n}|^2 dx$ dominates the energy, and s may become zero. In this case, defects are more likely to occur. (This heuristic argument is later confirmed in the numerical experiments.) Since the investigation of defects is of primary interest in this paper, we consider the most significant case to be $0 < \kappa < 1$.

We now describe our discretization $E_h[s_h,\mathbf{n}_h]$ of the energy (2.1) and its finite element minimizer $(s_h,\mathbf{n}_h)$.

2.2. Discretization of the energy. Let $\mathcal{T}_h = \{T\}$ be a conforming simplicial triangulation of the domain Ω. We denote by $\mathcal{N}_h$ the set of nodes (vertices) of $\mathcal{T}_h$ and the cardinality of $\mathcal{N}_h$ by N (with some abuse of notation). We demand that $\mathcal{T}_h$ be *weakly acute*, namely

$$k_{ij} := -\int_\Omega \nabla\phi_i \cdot \nabla\phi_j dx \geq 0 \quad \text{for all } i \neq j, \tag{2.6}$$

where ϕ_i is the standard "hat" function associated with node $x_i \in \mathcal{N}_h$. We indicate with $\omega_i = \operatorname{supp}\ \phi_i$ the patch of a node x_i (i.e. the "star" of elements in $\mathcal{T}_h$ that contain the vertex x_i). Condition (2.6) imposes a severe geometric restriction on $\mathcal{T}_h$ [21, 43]. We recall the following characterization of (2.6) for $d = 2$.

Proposition 2.1 (weak acuteness in two dimensions). *For any pair of triangles T_1, T_2 in $\mathcal{T}_h$ that share a common edge e, let α_i be the angle in T_i opposite to e (for $i = 1, 2$). If $\alpha_1 + \alpha_2 \leq \pi$ for every edge e, then* (2.6) *holds.*

Generalizations of Proposition 2.1 to three dimensions, involving interior dihedral angles of tetrahedra, can be found in [29, 18].

We construct continuous piecewise affine spaces associated with the mesh, i.e.

$$\begin{aligned}
&\mathbb{S}_h := \{s_h \in H^1(\Omega) : s_h|_T \text{ is affine for all } T \in \mathcal{T}_h\},\\
&\mathbb{U}_h := \{\mathbf{u}_h \in H^1(\Omega)^d : \mathbf{u}_h|_T \text{ is affine in each component for all } T \in \mathcal{T}_h\},\\
&\mathbb{N}_h := \{\mathbf{n}_h \in \mathbb{U}_h : |\mathbf{n}_h(x_i)| = 1 \text{ for all nodes } x_i \in \mathcal{N}_h\}.
\end{aligned} \tag{2.7}$$

We also have the discrete spaces that include (Dirichlet) boundary conditions:

$$\mathbb{S}_h(\Gamma_s, g_h) := \{s_h \in \mathbb{S}_h : s_h|_{\Gamma_s} = g_h\}, \quad \mathbb{N}_h(\Gamma_{\mathbf{n}}, \mathbf{r}_h) := \{\mathbf{n}_h \in \mathbb{N}_h : \mathbf{n}_h|_{\Gamma_{\mathbf{n}}} = \mathbf{r}_h\}, \tag{2.8}$$

where $(g_h, \mathbf{r}_h)$ are the Lagrange interpolations of $(g, \mathbf{r})$ and g and $\mathbf{r}$ are the traces of some $W^1_\infty(\Omega)$ functions.

In order to motivate our discrete version of $E_1[s, \mathbf{n}]$, note that $\sum_{j=1}^N k_{ij} = 0$ for all $x_i \in \mathcal{N}_h$. Therefore, for piecewise linear $s_h = \sum_{i=1}^N s_h(x_i)\phi_i$, we have

$$\int_\Omega |\nabla s_h|^2 dx = -\sum_{i=1}^N k_{ii} s_h(x_i)^2 - \sum_{i,j=1, i\neq j}^N k_{ij} s_h(x_i) s_h(x_j),$$

whence, exploiting $k_{ii} = -\sum_{j\neq i} k_{ij}$ and the symmetry $k_{ij} = k_{ji}$, we get

$$\begin{aligned} \int_\Omega |\nabla s_h|^2 dx &= \sum_{i,j=1}^N k_{ij} s_h(x_i)\big(s_h(x_i) - s_h(x_j)\big) \\ &= \frac{1}{2}\sum_{i,j=1}^N k_{ij}\big(s_h(x_i) - s_h(x_j)\big)^2 = \frac{1}{2}\sum_{i,j=1}^N k_{ij}\big(\delta_{ij} s_h\big)^2, \end{aligned} \tag{2.9}$$

where we define

$$\delta_{ij} s_h := s_h(x_i) - s_h(x_j), \quad \delta_{ij}\mathbf{n}_h := \mathbf{n}_h(x_i) - \mathbf{n}_h(x_j). \tag{2.10}$$

With this in mind, we define the discrete energy using

$$E_1^h[s_h, \mathbf{n}_h] := \frac{\kappa}{2}\sum_{i,j=1}^N k_{ij}\left(\delta_{ij} s_h\right)^2 + \frac{1}{2}\sum_{i,j=1}^N k_{ij}\left(\frac{s_h(x_i)^2 + s_h(x_j)^2}{2}\right)|\delta_{ij}\mathbf{n}_h|^2, \tag{2.11}$$

and

$$E_2^h[s_h] := \int_\Omega \psi(s_h(x)) dx. \tag{2.12}$$

The second summation in (2.11) does *not* come from applying the standard discretization of $\int_\Omega s^2 |\nabla \mathbf{n}|^2 dx$ by piecewise linear elements. It turns out that this special form of the discrete energy allows us to handle the degenerate coefficient s^2 *without* regularization. Eventually, we seek an approximation $(s_h, \mathbf{n}_h) \in \mathbb{S}_h(\Gamma_s, g_h) \times \mathbb{N}_h(\Gamma_{\mathbf{n}}, \mathbf{r}_h)$ of the pair $(s, \mathbf{n})$ such that the discrete pair $(s_h, \mathbf{n}_h)$ minimizes the discrete version of the bulk energy (2.1) given by

$$E_h[s_h, \mathbf{n}_h] := E_1^h[s_h, \mathbf{n}_h] + E_2^h[s_h]. \tag{2.13}$$

The following result shows that definition (2.11) preserves the key structure (2.2) of [2, 32] at the discrete level, and turns out to be crucial for our analysis as well. We first introduce two discrete versions of the auxiliary vector field $\mathbf{u}$

$$\mathbf{u}_h := I_h[s_h \mathbf{n}_h] \in \mathbb{U}_h, \quad \widetilde{\mathbf{u}}_h := I_h[|s_h|\mathbf{n}_h] \in \mathbb{U}_h, \tag{2.14}$$

where I_h denotes the piecewise linear Lagrange interpolation operator on mesh $\mathcal{T}_h$.

LEMMA 2.2 (energy inequality). *Let the mesh $\mathcal{T}_h$ satisfy* (2.6). *If $(s_h, \mathbf{n}_h) \in \mathbb{S}_h \times \mathbb{N}_h$, then, for any $\kappa > 0$, the discrete energy* (2.11) *satisfies*

$$E_1^h[s_h, \mathbf{n}_h] \geq (\kappa - 1)\int_\Omega |\nabla s_h|^2 dx + \int_\Omega |\nabla \mathbf{u}_h|^2 dx =: \widetilde{E}_1^h[s_h, \mathbf{u}_h], \tag{2.15}$$

as well as

$$E_1^h[s_h,\mathbf{n}_h] \geq (\kappa-1)\int_\Omega |\nabla I_h|s_h||^2dx + \int_\Omega |\nabla\widetilde{\mathbf{u}}_h|^2dx =: \widetilde{E}_1^h[I_h|s_h|,\widetilde{\mathbf{u}}_h]. \tag{2.16}$$

Proof. Since

$$\begin{aligned} s_h(x_i)\mathbf{n}_h(x_i) - s_h(x_j)\mathbf{n}_h(x_j) = {} & \frac{s_h(x_i)+s_h(x_j)}{2}\big(\mathbf{n}_h(x_i)-\mathbf{n}_h(x_j)\big) \\ & + \big(s_h(x_i)-s_h(x_j)\big)\frac{\mathbf{n}_h(x_i)+\mathbf{n}_h(x_j)}{2}, \end{aligned}$$

using the orthogonality relation $\big(\mathbf{n}_h(x_i)-\mathbf{n}_h(x_j)\big)\cdot\big(\mathbf{n}_h(x_i)+\mathbf{n}_h(x_j)\big) = |\mathbf{n}_h(x_i)|^2 - |\mathbf{n}_h(x_j)|^2 = 0$ and (2.9) yields

$$\begin{aligned} \int_\Omega |\nabla\mathbf{u}_h|^2dx &= \frac{1}{2}\sum_{i,j=1}^N k_{ij}|s_h(x_i)\mathbf{n}_h(x_i) - s_h(x_j)\mathbf{n}_h(x_j)|^2 \\ &= \frac{1}{2}\sum_{i,j=1}^N k_{ij}\left(\frac{s_h(x_i)+s_h(x_j)}{2}\right)^2|\delta_{ij}\mathbf{n}_h|^2 + \frac{1}{2}\sum_{i,j=1}^N k_{ij}(\delta_{ij}s_h)^2\left|\frac{\mathbf{n}_h(x_i)+\mathbf{n}_h(x_j)}{2}\right|^2. \end{aligned}$$

Employing again this orthogonality, this time in the form $|\mathbf{n}_h(x_i)-\mathbf{n}_h(x_j)|^2+|\mathbf{n}_h(x_i)+\mathbf{n}_h(x_j)|^2 = 4$, we obtain

$$\begin{aligned} \int_\Omega |\nabla\mathbf{u}_h|^2dx = {} & \frac{1}{2}\sum_{i,j=1}^N k_{ij}\left(\frac{s_h(x_i)+s_h(x_j)}{2}\right)^2|\delta_{ij}\mathbf{n}_h|^2 \\ & + \frac{1}{2}\sum_{i,j=1}^N k_{ij}(\delta_{ij}s_h)^2 - \frac{1}{2}\sum_{i,j=1}^N k_{ij}(\delta_{ij}s_h)^2\left|\frac{\mathbf{n}_h(x_i)-\mathbf{n}_h(x_j)}{2}\right|^2. \end{aligned} \tag{2.17}$$

Since $\big(s_h(x_i)+s_h(x_j)\big)^2 = \big(s_h(x_i)^2+s_h(x_j)^2\big) - \big(s_h(x_i)-s_h(x_j)\big)^2$, we infer that

$$E_1^h[s_h,\mathbf{n}_h] = \int_\Omega (\kappa-1)|\nabla s_h|^2 + |\nabla\mathbf{u}_h|^2dx + \sum_{i,j=1}^N k_{ij}(\delta_{ij}s_h)^2\left|\frac{\delta_{ij}\mathbf{n}_h}{2}\right|^2. \tag{2.18}$$

The inequality (2.15) follows directly from $k_{ij}\geq 0$ for $i\neq j$.

To prove (2.16), we note that the argument above still holds if we replace $\mathbf{u}_h$ with $\widetilde{\mathbf{u}}_h$ and s_h with $|s_h|$ to get

$$\int_\Omega |\nabla\widetilde{\mathbf{u}}_h|^2dx \leq \frac{1}{2}\sum_{i,j=1}^N k_{ij}\frac{s_h(x_i)^2+s_h(x_j)^2}{2}|\delta_{ij}\mathbf{n}_h|^2 + \frac{1}{2}\sum_{i,j=1}^N k_{ij}(\delta_{ij}|s_h|)^2. \tag{2.19}$$

We finally find that

$$\begin{aligned} \int_\Omega |\nabla\widetilde{\mathbf{u}}_h|^2dx + (\kappa-1)\int_\Omega |\nabla I_h|s_h||^2dx &= \int_\Omega |\nabla\widetilde{\mathbf{u}}_h|^2dx + \frac{\kappa-1}{2}\sum_{i,j=1}^N k_{ij}(\delta_{ij}|s_h|)^2 \\ &\leq \frac{1}{2}\sum_{i,j=1}^N k_{ij}\frac{s_h(x_i)^2+s_h(x_j)^2}{2}|\delta_{ij}\mathbf{n}_h|^2 + \frac{\kappa}{2}\sum_{i,j=1}^N k_{ij}(\delta_{ij}|s_h|)^2 \leq E_1^h[s_h,\mathbf{n}_h], \end{aligned}$$

where we have used the triangle inequality $\big(|s_h(x_i)|-|s_h(x_j)|\big)^2 \le \big(s_h(x_i)-s_h(x_j)\big)^2$. This completes the proof. □

REMARK 2.3 (purpose of (2.16)). *The presence of the Lagrange interpolation operator* I_h *in* (2.16) *might seem strange, but accounts for the variational crime committed when enforcing* $\widetilde{\mathbf{u}}_h = |s_h|\mathbf{n}_h$ only at the vertices. *This is necessary to prove the* Γ*-convergence of our discrete energy* (2.11) *to the original continuous energy in* (2.1). *In fact, we later exploit the weak lower semicontinuity in* $H^1(\Omega)$ *of* $\widetilde{E}_1^h[I_h|s_h|,\widetilde{\mathbf{u}}_h]$ *in* (2.16) *(Lemma 3.4 below), which is a consequence of its convexity with respect to* $\nabla\widetilde{\mathbf{u}}_h$. *This is not obvious when* $\kappa<1$, *the most significant case for formation of defects.*

3. Γ-convergence of the discrete energy. In this section, we show that our discrete energy (2.11) converges to the continuous energy (2.1) in the sense of Γ-convergence. Let the product space $\mathbb{X} := L^2(\Omega)\times L^2(\Omega)^d$ be equipped with the L^2-norm and let $\mathbb{X}_h := \mathbb{S}_h \times \mathbb{N}_h$. We define $E[s,\mathbf{n}]$ as in (2.1) for $(s,\mathbf{n})\in\mathcal{A}$ and $E[s,\mathbf{n}]=\infty$ for $(s,\mathbf{n})\in\mathbb{X}\setminus\mathcal{A}$. Likewise, we define $E_1^h[s_h,\mathbf{n}_h]$ as in (2.11) for $(s_h,\mathbf{n}_h)\in\mathbb{X}_h$ and $E_1^h[s,\mathbf{n}]=\infty$ for all $(s,\mathbf{n})\in\mathbb{X}\setminus\mathbb{X}_h$.

THEOREM 3.1 (Γ-convergence). *Let* $\{\mathcal{T}_h\}$ *be a sequence of weakly acute meshes. Then, for every* $(s,\mathbf{n})\in\mathbb{X}$ *the following two properties hold:*

- *Lim-inf inequality: for every sequence* $\{(s_h,\mathbf{n}_h)\}$ *converging strongly to* $(s,\mathbf{n})$ *in* $\mathbb{X}$*, we have*

$$E_1[s,\mathbf{n}] \le \liminf_{h\to 0} E_1^h[s_h,\mathbf{n}_h]; \tag{3.1}$$

- *Lim-sup inequality: there exists a sequence* $\{(s_h,\mathbf{n}_h)\}$ *such that* $(s_h,\mathbf{n}_h)$ *converges strongly to* $(s,\mathbf{n})$ *in* $\mathbb{X}$ *and*

$$E_1[s,\mathbf{n}] \ge \limsup_{h\to 0} E_1^h[s_h,\mathbf{n}_h]. \tag{3.2}$$

The proof of this theorem is split into several lemmas. We start with the lim-sup inequality (or consistency). We first observe that if $E_1(s,\mathbf{n})=\infty$, then the assertion (3.2) is valid for any sequence $(s_h,\mathbf{n}_h)$. Consequently, we consider the nontrivial case $E_1(s,\mathbf{n}) = \widetilde{E}_1[s,\mathbf{u}] < \infty$ or equivalently $(s,\mathbf{n})\in\mathcal{A}$. Since H^2-functions are dense in $\mathcal{A}$, given $\epsilon>0$ there exists $(s_\epsilon,\mathbf{u}_\epsilon)\in H^2(\Omega)\times H^2(\Omega)^d$ such that

$$\|(s,\mathbf{u})-(s_\epsilon,\mathbf{u}_\epsilon)\|_{H^1(\Omega)} \le \epsilon \quad \Rightarrow \quad \big|\widetilde{E}[s,\mathbf{u}]-\widetilde{E}[s_\epsilon,\mathbf{u}_\epsilon]\big| \le C\epsilon.$$

Therefore, we can assume that $(s,\mathbf{u})\in H^2(\Omega)^{1+d}$ for $d=2,3$, and let $(s_h,\mathbf{u}_h)$ be the Lagrange interpolants of $(s,\mathbf{u})$, which are well defined because $H^2(\Omega)\subset C^0(\overline{\Omega})$. Since $(s_h,\mathbf{u}_h)\to(s,\mathbf{u})$ in $H^1(\Omega)$, in view of the energy identity (2.18), we must show

$$\sum_{i,j=1}^N k_{ij}\big(\delta_{ij}s_h\big)^2\big|\delta_{ij}\mathbf{n}_h\big|^2 \to 0, \qquad \text{as } h\to 0. \tag{3.3}$$

Heuristically, if $\mathbf{n}(x)$ is smooth, then the sum (3.3) is of order $h^2\int_\Omega|\nabla s_h|^2dx$ which obviously converges to zero. However, such an argument fails if the director field $\mathbf{n}(x)$ lacks high regularity, which is the case with defects. These are discontinuities of $\mathbf{n}(x)$ which occur in the singular set $\mathcal{S}$ defined in (2.5). Since $\mathbf{n}(x)$ is not regular in general, the proof of consistency requires a separate treatment of the region where $\mathbf{n}(x)$ is regular and the region where $\mathbf{n}(x)$ is singular. The heuristic argument can be carried out in the regular region, while in the singular region we appeal to basic measure theory. With this motivation in mind, we now prove the following lemma.

LEMMA 3.2 (lim-sup inequality). *Let the pair* $(s,\mathbf{n})$ *belong to the admissible class* $\mathcal{A}$ *and* $(s,\mathbf{u}) \in H^2(\Omega)^{1+d}$. *If* $(s_h,\mathbf{u}_h)$ *are the Lagrange interpolants of* $(s,\mathbf{u})$, *then* $\widetilde{E}_1^h[s_h,\mathbf{u}_h] \to \widetilde{E}_1[s,\mathbf{u}]$ *as* $h \to 0$.

Proof. Given $\epsilon > 0$, we divide the domain Ω into two regions, $\mathcal{S}_\epsilon = \{x \in \Omega,\ |s(x)| < \epsilon\}$ and $\mathcal{K}_\epsilon = \overline{\Omega} \setminus \mathcal{S}_\epsilon$, and the sum in (3.3) into two parts

$$\mathcal{I}_h(\mathcal{K}_\epsilon) := \sum_{x_i,x_j \in \mathcal{K}_\epsilon} k_{ij}\big(\delta_{ij}s_h\big)^2\big|\delta_{ij}\mathbf{n}_h\big|^2, \quad \mathcal{I}_h(\mathcal{S}_\epsilon) := \sum_{x_i \text{ or } x_j \in \mathcal{S}_\epsilon} k_{ij}\big(\delta_{ij}s_h\big)^2\big|\delta_{ij}\mathbf{n}_h\big|^2,$$

where $\mathbf{n}_h(x_i) = \mathbf{n}(x_i)$ is well defined provided $s(x_i) \neq 0$ and otherwise $\mathbf{n}_h(x_i)$ is an arbitrary vector of unit length; thus $\mathbf{n}_h \in \mathbb{N}_h$.

Step 1: Estimate on $\mathcal{K}_\epsilon$. Note that $\mathcal{K}_\epsilon$ is a compact set. Since $\mathbf{n} = s^{-1}\mathbf{u}$ is continuous everywhere except on the singular set $\mathcal{S}$, the field $\mathbf{n}$ is uniformly continuous on $\mathcal{K}_\epsilon$. Thus, we have $|\mathbf{n}_h(x_i) - \mathbf{n}_h(x_j)| \to 0$ uniformly as the meshsize $h \to 0$ because x_i and x_j are connected by a single edge of the mesh. Therefore, as $h \to 0$

$$\mathcal{I}_h(\mathcal{K}_\epsilon) \le \left(\max_{\substack{x_i,x_j \in \mathcal{K}_\epsilon, \\ |x_i - x_j| \le h}} |\mathbf{n}_h(x_i) - \mathbf{n}_h(x_j)|^2 \right) \sum_{i,j=1}^{N} k_{ij}(\delta_{ij}s_h)^2 = o(1) \int_\Omega |\nabla s_h|^2 dx \to 0.$$

Step 2: Estimate on $\mathcal{S}_\epsilon$. If either x_i or x_j is in $\mathcal{S}_\epsilon$, without loss of generality, we assume that $x_i \in \mathcal{S}_\epsilon$. Since $s(x)$ is uniformly continuous, and $s_h(x)$ is the Lagrange interpolant of $s(x)$, there is a meshsize h such that for any x in the star ω_i of x_i, $|s_h(x) - s_h(x_i)| \le \epsilon$, which implies that $\omega_i \subset \mathcal{S}_{2\epsilon}$. Thus, by the triangle inequality,

$$\mathcal{I}_h(\mathcal{S}_\epsilon) \le 4 \sum_{x_i \text{ or } x_j \in \mathcal{S}_\epsilon} k_{ij}(\delta_{ij}s_h)^2 \le 8 \int_{\cup\,\omega_i} |\nabla s_h|^2 dx \le 8 \int_{\mathcal{S}_{2\epsilon}} |\nabla s_h|^2 dx,$$

where the union $\cup\,\omega_i$ is taken over all nodes x_i in $\mathcal{S}_\epsilon$. Since $s \in H^2(\Omega)$, we have

$$\int_{\mathcal{S}_{2\epsilon}} |\nabla s_h|^2 dx \to \int_{\mathcal{S}_{2\epsilon}} |\nabla s|^2 dx \quad \text{as } h \to 0.$$

Step 3: The limit $\epsilon \to 0$. Combining Steps 1 and 2 gives

$$\lim_{h \to 0} \sum_{i,j=1}^{N} k_{ij}\big(\delta_{ij}s_h\big)^2\big|\delta_{ij}\mathbf{n}_h\big|^2 \le 8 \int_{\mathcal{S}_{2\epsilon}} |\nabla s|^2 dx,$$

for all $\epsilon > 0$. We finally show that

$$\int_{\mathcal{S}_{2\epsilon}} |\nabla s|^2 dx = \int_\Omega |\nabla s|^2 \chi_{\{|s| \le 2\epsilon\}} dx \to 0 \quad \text{as } \epsilon \to 0,$$

where χ_A is the characteristic function of the set A. By virtue of the Lebesgue's dominated convergence theorem, we obtain

$$\lim_{\epsilon \to 0} \int_\Omega |\nabla s|^2 \chi_{\{|s| \le 2\epsilon\}} dx = \int_\Omega |\nabla s|^2 \chi_{\{s=0\}} dx = 0,$$

where the last equality follows by basic measure theory, i.e. $\nabla s(x) = \mathbf{0}$ for a.e. x in $\{s(x) = 0\}$ [26, Ch. 5, exercise 17, p. 292.]. This proves the lemma. ◻

To prove the lim-inf inequality (3.1), we need first to show coercivity (Lemma 3.3) and weak lower semi-continuity (Lemma 3.4). We do this next.

Lemma 3.3 (coercivity). *For any* $(s_h, \mathbf{n}_h) \in \mathbb{S}_h \times \mathbb{N}_h$, *we have*

$$E_1^h[s_h, \mathbf{n}_h] \geq \min\{\kappa, 1\} \int_\Omega |\nabla \widetilde{\mathbf{u}}_h|^2 dx \geq \min\{\kappa, 1\} \int_\Omega |\nabla I_h |s_h||^2 dx.$$

Proof. Inequality (2.16) of Lemma 2.2 shows that

$$E_1^h[s_h, \mathbf{n}_h] \geq (\kappa - 1) \int_\Omega |\nabla I_h |s_h||^2 dx + \int_\Omega |\nabla \widetilde{\mathbf{u}}_h|^2 dx. \tag{3.4}$$

If $\kappa \geq 1$, then $E_1^h[s_h, \mathbf{n}_h]$ obviously controls the H^1-norm of $\widetilde{\mathbf{u}}_h$ with constant 1.

If $0 < \kappa < 1$, then combining (2.11) with (2.19) yields

$$\begin{aligned} E_1^h[s_h, \mathbf{n}_h] &\geq \frac{\kappa}{2} \sum_{i,j=1}^N k_{ij} \left(\delta_{ij} |s_h|\right)^2 + \frac{\kappa}{2} \sum_{i,j=1}^N k_{ij} \left(\frac{s_h(x_i)^2 + s_h(x_j)^2}{2} \right) |\delta_{ij} \mathbf{n}_h|^2 \\ &\geq \kappa \int_\Omega |\nabla \widetilde{\mathbf{u}}_h|^2 dx, \end{aligned}$$

whence $E_1^h[s_h, \mathbf{n}_h] \geq \min\{\kappa, 1\} \int_\Omega |\nabla \widetilde{\mathbf{u}}_h|^2 dx$ as asserted. Since

$$\sum_{i,j=1}^N k_{ij} \left|\widetilde{\mathbf{u}}_h(x_i) - \widetilde{\mathbf{u}}_h(x_j)\right|^2 \geq \sum_{i,j=1}^N k_{ij} \left(|\widetilde{\mathbf{u}}_h(x_i)| - |\widetilde{\mathbf{u}}_h(x_j)|\right)^2,$$

and $|s_h(x_i)| = |\widetilde{\mathbf{u}}_h(x_i)|$ for all nodes, we obtain

$$\int_\Omega |\nabla \widetilde{\mathbf{u}}_h|^2 dx \geq \int_\Omega |\nabla I_h |\widetilde{\mathbf{u}}_h||^2 dx = \int_\Omega |\nabla I_h |s_h||^2 dx,$$

which is the desired second estimate. □

Weak lower semi-continuity usually follows from convexity. While it is obvious that the discrete energy $\widetilde{E}_1[s_h, \mathbf{u}_h]$ in (2.15) is convex with respect to $\nabla \mathbf{u}_h$ and ∇s_h if $\kappa \geq 1$, the convexity is not clear if $0 < \kappa < 1$. It is worth mentioning that if $\kappa < 1$, the convexity of the continuous energy (2.2) is based on the fact that $|\mathbf{u}| = |s|$ a.e. in Ω and hence the convex part $\int_\Omega |\nabla \mathbf{u}|^2 dx$ controls the concave part $(\kappa - 1) \int_\Omega |\nabla s|^2 dx$ [32]. However, for the discrete energy (2.15), the equality $|\mathbf{u}_h| = |s_h|$ holds only at the vertices. Therefore, it is nontrivial to establish the weak lower semi-continuity of $\widetilde{E}_1^h[s_h, \mathbf{u}_h]$. This is why we exploit the nodal relation $|s_h| = |\mathbf{u}_h|$ to derive an alternative formula for $\widetilde{E}_1^h[I_h|s_h|, \widetilde{\mathbf{u}}_h]$. Our next lemma hinges on (2.16) and makes the convexity of $\widetilde{E}_1^h[I_h|s_h|, \widetilde{\mathbf{u}}_h]$ with respect to $\nabla \widetilde{\mathbf{u}}_h$ completely explicit.

Lemma 3.4 (weak lower semi-continuity). *The energy* $\int_\Omega L_h(\mathbf{w}_h, \nabla \mathbf{w}_h) dx$, *with*

$$L_h(\mathbf{w}_h, \nabla \mathbf{w}_h) := (\kappa - 1) |\nabla I_h |\mathbf{w}_h||^2 + |\nabla \mathbf{w}_h|^2,$$

is well defined for any $\mathbf{w}_h \in \mathbb{U}_h$ *and is weakly lower semi-continuous in* $H^1(\Omega)$, *i.e. for any weakly convergent sequence* $\mathbf{w}_h \rightharpoonup \mathbf{w}$ *in the* H^1 *norm, we have*

$$\liminf_{h \to 0} \int_\Omega L_h(\mathbf{w}_h, \nabla \mathbf{w}_h) dx \geq \int_\Omega (\kappa - 1) |\nabla |\mathbf{w}||^2 + |\nabla \mathbf{w}|^2 dx.$$

Proof. If $\kappa \geq 1$, then the assertion follows from standard arguments. Here, we only dwell upon $0 < \kappa < 1$ and dimension $d = 2$, because the case $d = 3$ is similar. After extracting a subsequence (not relabeled) we can assume that $\mathbf{w}_h$ converges to $\mathbf{w}$ strongly in $L^2(\Omega)$ and pointwise a.e. in Ω.

Step 1: Equivalent form of L_h. We let T be any triangle in the mesh $\mathcal{T}_h$, label its three vertices as x_0, x_1, x_2, and define $\mathbf{e}_1 := x_1 - x_0$ and $\mathbf{e}_2 := x_2 - x_0$. After denoting $\mathbf{w}_h^i = \mathbf{w}_h(x_i)$ for $i = 0, 1, 2$, a simple calculation yields

$$\nabla \mathbf{w}_h = (\mathbf{w}_h^1 - \mathbf{w}_h^0) \otimes \mathbf{e}_1^* + (\mathbf{w}_h^2 - \mathbf{w}_h^0) \otimes \mathbf{e}_2^*,$$
$$\nabla I_h |\mathbf{w}_h| = (|\mathbf{w}_h^1| - |\mathbf{w}_h^0|)\mathbf{e}_1^* + (|\mathbf{w}_h^2| - |\mathbf{w}_h^0|)\mathbf{e}_2^*,$$

where $\{\mathbf{e}_i^*\}$ is the dual basis of $\{\mathbf{e}_i\}$, that is, $\mathbf{e}_i^* \cdot \mathbf{e}_j = I_{ij}$, and $I = (I_{ij})_{i,j=1}^2$ is the identity matrix. Assuming $|\mathbf{w}_h^i| + |\mathbf{w}_h^0| \neq 0$, we realize that

$$|\mathbf{w}_h^i| - |\mathbf{w}_h^0| = \frac{\mathbf{w}_h^i + \mathbf{w}_h^0}{|\mathbf{w}_h^i| + |\mathbf{w}_h^0|} \cdot (\mathbf{w}_h^i - \mathbf{w}_h^0).$$

We then obtain $\nabla I_h |\mathbf{w}_h| = G_h(\mathbf{w}_h) : \nabla \mathbf{w}_h$ where $G_h(\mathbf{w}_h)$ is the 3-tensor:

$$G_h(\mathbf{w}_h) := \frac{\mathbf{w}_h^1 + \mathbf{w}_h^0}{|\mathbf{w}_h^1| + |\mathbf{w}_h^0|} \otimes \mathbf{e}_1 \otimes \mathbf{e}_1^* + \frac{\mathbf{w}_h^2 + \mathbf{w}_h^0}{|\mathbf{w}_h^2| + |\mathbf{w}_h^0|} \otimes \mathbf{e}_2 \otimes \mathbf{e}_2^*, \quad \text{on } T,$$

and the contraction between a 3-tensor and a 2-tensor in dyadic form is given by

$$(\mathbf{g}_1 \otimes \mathbf{g}_2 \otimes \mathbf{g}_3) : (\mathbf{m}_1 \otimes \mathbf{m}_2) := (\mathbf{g}_1 \cdot \mathbf{m}_1)(\mathbf{g}_2 \cdot \mathbf{m}_2)\mathbf{g}_3.$$

Therefore, we have

$$L_h(\mathbf{w}_h, \nabla \mathbf{w}_h) = |\nabla \mathbf{w}_h|^2 + (\kappa - 1)|G_h(\mathbf{w}_h) : \nabla \mathbf{w}_h|^2,$$

which expresses $L_h(\mathbf{w}_h, \nabla \mathbf{w}_h)$ directly in terms of $\nabla \mathbf{w}_h$ and nodal values of $\mathbf{w}_h$.

Step 2: Convergence of $G_h(\mathbf{w}_h)$. Given $\epsilon > 0$, Egoroff's Theorem [48] asserts that

$$\mathbf{w}_h \to \mathbf{w} \quad \text{uniformly on } E_\epsilon,$$

for some subset E_ϵ and $|\Omega \backslash E_\epsilon| \leq \epsilon$. We now consider the set $A_\epsilon := \{|\mathbf{w}(x)| \geq 2\epsilon\} \cap E_\epsilon$, and observe that there exists a sufficiently small h_ϵ such that for any $x \in A_\epsilon$

$$|\mathbf{w}_h(x)| \geq \epsilon \quad \text{for all } h \leq h_\epsilon.$$

If $G(\mathbf{w}) := \frac{\mathbf{w}}{|\mathbf{w}|} \otimes I$, then we claim that

$$\int_{A_\epsilon} |G_h(\mathbf{w}_h) - G(\mathbf{w})|^2 dx \to 0, \quad \text{as } h \to 0. \tag{3.5}$$

For any $x \in A_\epsilon$, let $\{T_h\}$ be a sequence of triangles such that $x \in \overline{T_h}$. Since $|\mathbf{w}_h(x)| \geq \epsilon$ and $\mathbf{w}_h$ is piecewise linear, there exists a vertex of T_h, which we label as x_h^0, such that $|\mathbf{w}_h^0| \geq \epsilon$. To compare $G_h(\mathbf{w}_h)$ with $\frac{\mathbf{w}_h(x)}{|\mathbf{w}_h(x)|} \otimes I$, we use that $I = \mathbf{e}_1 \otimes \mathbf{e}_1^* + \mathbf{e}_2 \otimes \mathbf{e}_2^*$:

$$G_h(\mathbf{w}_h) - \frac{\mathbf{w}_h(x)}{|\mathbf{w}_h(x)|} \otimes I = \sum_{i=1,2} \left(\frac{\mathbf{w}_h^i + \mathbf{w}_h^0}{|\mathbf{w}_h^i| + |\mathbf{w}_h^0|} - \frac{\mathbf{w}_h(x)}{|\mathbf{w}_h(x)|} \right) \otimes \mathbf{e}_i \otimes \mathbf{e}_i^*.$$

We define $H(\mathbf{x},\mathbf{y}) := \frac{\mathbf{x}+\mathbf{y}}{|\mathbf{x}|+|\mathbf{y}|}$ and observe that for all $x \in A_\epsilon$, we have

$$G_h(\mathbf{w}_h) - \frac{\mathbf{w}_h(x)}{|\mathbf{w}_h(x)|} \otimes I = \sum_{i=1,2} \big(H(\mathbf{w}_h^0, \mathbf{w}_h^i) - H(\mathbf{w}_h(x), \mathbf{w}_h(x)) \big) \otimes \mathbf{e}_i \otimes \mathbf{e}_i^*.$$

Next, we estimate

$$\begin{aligned} |H(\mathbf{w}_h^0, \mathbf{w}_h^i) - H(\mathbf{w}_h(x), \mathbf{w}_h(x))| &= \left| \frac{|\mathbf{w}_h(x)|(\mathbf{w}_h^0 + \mathbf{w}_h^i) - (|\mathbf{w}_h^0| + |\mathbf{w}_h^i|)\mathbf{w}_h(x)}{(|\mathbf{w}_h^0| + |\mathbf{w}_h^i|)|\mathbf{w}_h(x)|} \right| \\ \le \left| \frac{\mathbf{w}_h^0 + \mathbf{w}_h^i - 2\mathbf{w}_h(x)}{|\mathbf{w}_h^0| + |\mathbf{w}_h^i|} \right| &+ \left| \frac{(|\mathbf{w}_h(x)| - |\mathbf{w}_h^0|)\mathbf{w}_h(x)}{(|\mathbf{w}_h^0| + |\mathbf{w}_h^i|)|\mathbf{w}_h(x)|} \right| + \left| \frac{(|\mathbf{w}_h(x)| - |\mathbf{w}_h^i|)\mathbf{w}_h(x)}{(|\mathbf{w}_h^0| + |\mathbf{w}_h^i|)|\mathbf{w}_h(x)|} \right|. \end{aligned}$$

Since $|\mathbf{w}_h^0|, |\mathbf{w}_h(x)| \ge \epsilon$, and $\mathbf{w}_h(x) - \mathbf{w}_h(x_h^i) = \nabla \mathbf{w}_h \cdot (x - x_h^i)$ for all $x \in \overline{T_h}$, we have

$$\big| H(\mathbf{w}_h^0, \mathbf{w}_h^i) - H(\mathbf{w}_h(x), \mathbf{w}_h(x)) \big| \le C \frac{h}{\epsilon} |\nabla \mathbf{w}_h| \quad \forall x \in A_\epsilon \cap \overline{T_h}.$$

Integrating on A_ϵ, we obtain

$$\int_{A_\epsilon} \left| G_h(\mathbf{w}_h) - \frac{\mathbf{w}_h(x)}{|\mathbf{w}_h(x)|} \otimes I \right|^2 dx \le C \frac{h^2}{\epsilon^2} \int_{A_\epsilon} |\nabla \mathbf{w}_h(x)|^2 dx \to 0, \quad \text{as } h \to 0.$$

Since $\mathbf{w}_h \to \mathbf{w}$ a.e. in Ω, and $\frac{\mathbf{w}_h}{|\mathbf{w}_h|} - \frac{\mathbf{w}}{|\mathbf{w}|}$ is bounded, applying the dominated convergence theorem, we infer that

$$\int_{A_\epsilon} \left| \frac{\mathbf{w}_h}{|\mathbf{w}_h|} - \frac{\mathbf{w}}{|\mathbf{w}|} \right|^2 \to 0, \quad \text{as } h \to 0.$$

Combining these two limits, we deduce (3.5).

Step 3: Convexity. We now prove that the energy density

$$L(\mathbf{w}, M) := |M|^2 + (\kappa - 1)|G(\mathbf{w}) : M|^2$$

is convex with respect to any matrix M for any vector $\mathbf{w}$. Note that $L(\mathbf{w}, M)$ is a quadratic function of M, so we only need to show that $L(\mathbf{w}, M) \ge 0$ for any M and $\mathbf{w}$. Thus, it suffices to show that $|G(\mathbf{w}) : M| \le |M|$.

Assume that $M = \sum_{i,j} m_{ij} \mathbf{v}_i \otimes \mathbf{v}_j$ where $\{\mathbf{v}_i\}_{i=1}^2$ is the canonical basis on $\mathbb{R}^2$. Then we have $|M|^2 = \sum_{i,j=1}^2 m_{ij}^2$ and a simple calculation yields

$$\begin{aligned} G(\mathbf{w}) : M &= \frac{\sum_i w_i \mathbf{v}_i}{|\mathbf{w}|} \otimes (\mathbf{v}_1 \otimes \mathbf{v}_1 + \mathbf{v}_2 \otimes \mathbf{v}_2) : \left(\sum_{k,l} m_{kl} \mathbf{v}_k \otimes \mathbf{v}_l \right) \\ &= \frac{1}{|\mathbf{w}|} \sum_{i,k,l} w_i m_{kl} \delta_{ik} \mathbf{v}_l = \frac{1}{|\mathbf{w}|} \sum_{i,l} w_i m_{il} \mathbf{v}_l, \end{aligned}$$

where $\mathbf{w} = \sum_{i=1}^2 w_i \mathbf{v}_i$. Therefore, we obtain

$$|G(\mathbf{w}) : M|^2 = \frac{1}{|\mathbf{w}|^2} \sum_{j=1}^2 \left(\sum_{i=1}^2 w_i m_{ij} \right)^2.$$

The Cauchy-Schwarz inequality yields

$$\left(\sum_{i=1}^{2} w_i m_{ij}\right)^2 \leq \left(\sum_{i=1}^{2} w_i^2\right)\left(\sum_{i=1}^{2} m_{ij}^2\right) = |\mathbf{w}|^2 \left(\sum_{i=1}^{2} m_{ij}^2\right),$$

which implies $|G(\mathbf{w}) : M|^2 \leq |M|^2$ and $L(\mathbf{w}, M) \geq 0$ for any matrix M and vector $\mathbf{w}$. A similar argument shows that $L_h(\mathbf{w}_h, M) \geq 0$ for any matrix M and vector $\mathbf{w}_h$.

Step 4: Weak lower semi-continuity. Since $G_h(\mathbf{w}_h) \to G(\mathbf{w})$ in $L^2(A_\epsilon)$ according to (3.5), Egoroff's theorem yields

$$G_h(\mathbf{w}_h) \to G(\mathbf{w}) \quad \text{uniformly on } B_\epsilon,$$

where $B_\epsilon \subset A_\epsilon$ and $|A_\epsilon \setminus B_\epsilon| \leq \epsilon$. We claim that

$$\liminf_{h\to 0} \int_\Omega L_h(\mathbf{w}_h, \nabla\mathbf{w}_h)dx \geq \int_{B_\epsilon} L(\mathbf{w}, \nabla\mathbf{w})dx. \tag{3.6}$$

Step 3 implies $L_h(\mathbf{w}_h, \nabla\mathbf{w}_h) \geq 0$ for all $x \in \Omega$. Hence,

$$\int_\Omega L_h(\mathbf{w}_h, \nabla\mathbf{w}_h)dx \geq \int_{B_\epsilon} \Big(|\nabla\mathbf{w}_h|^2 + (\kappa - 1)|G_h(\mathbf{w}_h) : \nabla\mathbf{w}_h|^2\Big)dx.$$

A simple calculation yields

$$\int_\Omega L_h(\mathbf{w}_h, \nabla\mathbf{w}_h)dx \geq \int_{B_\epsilon} L(\mathbf{w}, \nabla\mathbf{w}_h)dx + (\kappa - 1)Q_h(\mathbf{w}, \mathbf{w}_h)$$

where

$$\begin{aligned} Q_h(\mathbf{w}, \mathbf{w}_h) := \int_{B_\epsilon} \Big(&[(G_h(\mathbf{w}_h) - G(\mathbf{w})) : \nabla\mathbf{w}_h]^t [G_h(\mathbf{w}_h) : \nabla\mathbf{w}_h] \\ &+ (G(\mathbf{w}) : \nabla\mathbf{w}_h)^t [(G_h(\mathbf{w}_h) - G(\mathbf{w})) : \nabla\mathbf{w}_h]\Big)dx. \end{aligned}$$

Since $L(\mathbf{w}, \nabla\mathbf{w}_h)$ is convex with respect to $\nabla\mathbf{w}_h$ (Step 3), we have [26, pg. 446, Sec. 8.2.2]

$$\liminf_{h\to 0} \int_{B_\epsilon} L(\mathbf{w}, \nabla\mathbf{w}_h)dx \geq \int_{B_\epsilon} L(\mathbf{w}, \nabla\mathbf{w})dx.$$

To prove (3.6), it remains to show that $Q_h(\mathbf{w}, \mathbf{w}_h) \to 0$ as $h \to 0$. Since $G(\mathbf{w})$ and $G_h(\mathbf{w}_h)$ are bounded and $\int_\Omega |\nabla\mathbf{w}_h(x)|^2 dx$ is uniformly bounded, we have

$$\begin{aligned} Q_h(\mathbf{w}, \mathbf{w}_h) &\leq C \int_{B_\epsilon} |G_h(\mathbf{w}_h) - G(\mathbf{w})||\nabla\mathbf{w}_h|^2 dx \\ &\leq C \max_{B_\epsilon} \big|G_h(\mathbf{w}_h) - G(\mathbf{w})\big| \int_{B_\epsilon} |\nabla\mathbf{w}_h|^2 dx \to 0 \quad \text{as } h \to 0, \end{aligned}$$

due to the uniform convergence of $G_h(\mathbf{w}_h)$ to $G(\mathbf{w})$ in B_ϵ. Therefore, we infer that $\liminf_{h\to 0} \int_\Omega L_h(\mathbf{w}_h, \nabla\mathbf{w}_h)dx \geq \int_{B_\epsilon} L(\mathbf{w}, \nabla\mathbf{w})dx$.

Since the inequality above holds for arbitrarily small ϵ, taking $\epsilon \to 0$ yields

$$\liminf_{h\to 0} \int_\Omega L_h(\mathbf{w}_h, \nabla\mathbf{w}_h)dx \geq \int_{\Omega\setminus\{\mathbf{w}(x)=0\}} L(\mathbf{w}, \nabla\mathbf{w})dx = \int_\Omega L(\mathbf{w}, \nabla\mathbf{w})dx,$$

where the last equality follows from $\nabla \mathbf{w} = \mathbf{0}$ a.e. in the set $\{\mathbf{w}(x) = \mathbf{0}\}$ [26, Ch. 5, exercise 17, p. 292.]. Finally, noting that $G(\mathbf{w}) : \nabla \mathbf{w} = \nabla |\mathbf{w}|$, we get the assertion. □

LEMMA 3.5 (characterizing limits). *Let $\{\mathcal{T}_h\}$ satisfy (2.6) and let $(s_h, \mathbf{n}_h) \in \mathbb{X}_h$ converge strongly to $(s, \mathbf{n}) \in \mathbb{X}$. Suppose that there exists a constant $C > 0$ such that*

$$E_1^h(s_h, \mathbf{n}_h) \leq C \quad \textit{for all } h > 0, \tag{3.7}$$

and let $\mathbf{u}_h, \widetilde{\mathbf{u}}_h \in \mathbb{U}_h$ be defined in (2.14). Then $(s, \mathbf{n}) \in \mathcal{A}$ and there is a subsequence $\{(I_h|s_h|, \widetilde{\mathbf{u}}_h)\}$ (not relabeled) that converges weakly in $H^1(\Omega)$, strongly in $L^2(\Omega)$, and pointwise a.e. to $(|s|, \widetilde{\mathbf{u}})$, where $\widetilde{\mathbf{u}} = |s|\mathbf{n}$. In addition, there is also a subsequence $\{(s_h, \mathbf{u}_h)\}$ (not relabeled) that converges weakly in $H^1(\Omega)$, strongly in $L^2(\Omega)$, and pointwise a.e. to $(s, \mathbf{u})$, where $\mathbf{u} = s\mathbf{n}$.

Proof. We define $\widetilde{s}_h := I_h|s_h|$ and use Lemma 3.3 (coercivity) in conjunction with (3.7) to realize that the H^1-norm of $(\widetilde{s}_h, \widetilde{\mathbf{u}}_h)$ is uniformly bounded in h. We can thus extract a subsequence (not relabeled) converging weakly in $H^1(\Omega)$, strongly in $L^2(\Omega)$, and pointwise a.e. to $(\widetilde{s}, \widetilde{\mathbf{u}}) \in H^{1+d}(\Omega)$. We must relate this limit to $(s, \mathbf{n})$.

Since $s_h \to s$ in $L^2(\Omega)$, s_h and $|s_h|$ converge pointwise a.e. to s and $|s|$. Moreover,

$$\|\widetilde{s}_h - |s_h|\|_{L^2(\Omega)} = \|I_h|s_h| - |s_h|\|_{L^2(\Omega)} \leq Ch\|\nabla |s_h|\|_{L^2(\Omega)} \leq Ch\|\nabla s_h\|_{L^2(\Omega)},$$

where $\|\nabla s_h\|_{L^2(\Omega)}$ is uniformly bounded because of (3.7) as well as (2.9) and (2.11). Consequently, $|s| = \widetilde{s} \in H^1(\Omega)$ and so $s \in H^1(\Omega)$ as well.

Next, we show that $\widetilde{\mathbf{u}} = |s|\mathbf{n}$. Since $\widetilde{s}_h$ and $\mathbf{n}_h$ are piecewise linear functions over $\mathcal{T}_h$, we observe that

$$\|\widetilde{s}_h\mathbf{n}_h - I_h[\widetilde{s}_h\mathbf{n}_h]\|_{L^1(\Omega)} \leq Ch^2\|\nabla\widetilde{s}_h \otimes \nabla\mathbf{n}_h\|_{L^1(\Omega)} \leq Ch^2\|\nabla\widetilde{s}_h\|_{L^2(\Omega)}\|\nabla\mathbf{n}_h\|_{L^2(\Omega)}.$$

An inverse estimate shows that $\|\nabla\mathbf{n}_h\|_{L^2(\Omega)} \leq Ch^{-1}|\Omega|^{1/2}$ because $|\mathbf{n}_h| \leq 1$. Hence, $\|\widetilde{s}_h\mathbf{n}_h - I_h[\widetilde{s}_h\mathbf{n}_h]\|_{L^1(\Omega)} = O(h)$. Now write

$$\widetilde{\mathbf{u}}_h - |s|\mathbf{n} = (I_h[\widetilde{s}_h\mathbf{n}_h] - \widetilde{s}_h\mathbf{n}_h) + (\widetilde{s}_h\mathbf{n}_h - |s|\mathbf{n}),$$

and note that the first term goes to zero in $L^1(\Omega)$ with rate h and the second one goes to zero in $L^1(\Omega)$ because $(\widetilde{s}_h, \mathbf{n}_h)$ converges to $(|s|, \mathbf{n})$ in $L^2(\Omega)$; ergo, $\widetilde{\mathbf{u}} = |s|\mathbf{n}$.

Since $\|\nabla s_h\|_{L^2(\Omega)} \leq C$, (3.7) together with (2.15) gives $\|\nabla\mathbf{u}_h\|_{L^2(\Omega)} \leq C$. The preceding argument thus shows that a subsequence of $\mathbf{u}_h$ converges weakly in $H^1(\Omega)$, strongly in $L^2(\Omega)$ and pointwise a.e. to $\mathbf{u} = s\mathbf{n} \in H^1(\Omega)^d$.

We finally prove that $|\mathbf{n}| = 1$ a.e. in Ω, which implies $(s, \mathbf{n}) \in \mathcal{A}$. We first observe that $I_h|\widetilde{\mathbf{u}}_h| = I_h|s_h|$ along with

$$\||\widetilde{\mathbf{u}}_h| - I_h|\widetilde{\mathbf{u}}_h|\|_{L^2(\Omega)} \leq Ch\|\nabla|\widetilde{\mathbf{u}}_h|\|_{L^2(\Omega)} \leq Ch\|\nabla\widetilde{\mathbf{u}}_h\|_{L^2(\Omega)} \leq Ch.$$

Since $I_h|s_h| \to |s|$ and $I_h|\widetilde{\mathbf{u}}_h| \to |\widetilde{\mathbf{u}}|$ as $h \to 0$, we deduce that $|s| = |\widetilde{\mathbf{u}}|$ a.e. in Ω, or equivalently $|\mathbf{n}| = 1$ a.e. in Ω as asserted. □

We now prove the main theorem.

Proof of Theorem 3.1. he lim-sup inequality (3.2) follows directly from Lemma 3.2 provided $(s, \mathbf{n}) \in \mathcal{A}$; otherwise $E[s, \mathbf{n}] = \infty$ and (3.2) is obvious.

As for the lim-inf inequality (3.1), let $(s, \mathbf{n}) \in \mathbb{X}$ and take $\{(s_h, \mathbf{n}_h) \in \mathbb{X}_h\}$ to be any sequence that converges to $(s, \mathbf{n})$ in the L^2-norm. If $\liminf_{h\to 0} E_1^h(s_h, \mathbf{n}_h) = \infty$, then there is nothing to prove. So assume that $E_1^h(s_h, \mathbf{n}_h)$ is uniformly bounded for a subsequence (not relabeled). By Lemma 3.5, $(s, \mathbf{n}) \in \mathcal{A}$ is an admissible pair and there exists a subsequence $(I_h|s_h|, \widetilde{\mathbf{u}}_h)$ converging weakly in H^1, strongly in L^2 and pointwise a.e. to $(|s|, \widetilde{\mathbf{u}})$ with $\widetilde{\mathbf{u}} = |s|\mathbf{n}$. Since $I_h|s_h| = I_h|\widetilde{\mathbf{u}}_h|$, invoking (2.16) in conjunction with Lemma 3.4 (weak lower semi-continuity), we obtain

$$\liminf_{h\to 0} E_1^h[s_h, \mathbf{n}_h] \geq \int_\Omega (\kappa - 1)|\nabla|\widetilde{\mathbf{u}}||^2 + |\nabla\widetilde{\mathbf{u}}|^2 dx.$$

Exploiting the properties $\widetilde{\mathbf{u}} = |s|\mathbf{n}$ and $|\mathbf{n}| = 1$ a.e. in Ω, we deduce the orthogonal decomposition $\nabla\widetilde{\mathbf{u}} = \nabla|s| \otimes \mathbf{n} + |s|\nabla\mathbf{n}$ a.e. in Ω. Hence,

$$\begin{aligned}\int_\Omega (\kappa - 1)|\nabla|\widetilde{\mathbf{u}}||^2 + |\nabla\widetilde{\mathbf{u}}|^2 dx &= \int_\Omega \kappa|\nabla|s||^2 + |s|^2|\nabla\mathbf{n}|^2 dx \\ &= \int_\Omega \kappa|\nabla s|^2 + s^2|\nabla\mathbf{n}|^2 dx \equiv E_1[s, \mathbf{n}].\end{aligned}$$

This completes the proof. □

The Γ-convergence result immediately yields the following corollary [17, 23].

Corollary 3.6 (convergence of global discrete minimizers). *Let $\{\mathcal{T}_h\}$ satisfy (2.6). If $\{(s_n, \mathbf{n}_h)\} \subset \mathbb{X}_h$ is a sequence of global minimizers of the discrete energy $E_h[s_h, \mathbf{n}_h]$ in (2.13), then there is a subsequence that converges weakly in $H^1(\Omega)$, strongly in $L^2(\Omega)$, and pointwise a.e. in Ω to an admissible pair $(s, \mathbf{n}) \in \mathcal{A}$, which is a global minimizer of the continuous energy $E[s, \mathbf{n}]$ in (2.1). In addition,*

$$E_h[s_h, \mathbf{n}_h] \to E[s, \mathbf{n}] \quad \text{as } h \to 0.$$

This corollary is about global minimizers, both discrete and continuous. In the next section, we design a quasi-gradient flow to compute discrete local minimizers, and show its convergence (see Theorem 4.2). In general, convergence to a global minimizer is not available, nor are rates of convergence due to the lack of continuous dependence results. However, if local minimizers of $E[s, \mathbf{n}]$ are isolated, then there exists local minimizers of $E_h[s_h, \mathbf{n}_h]$ that Γ-converge to $(s, \mathbf{n})$ [17, 23].

4. Quasi-Gradient Flow. We consider a gradient flow methodology consisting of a gradient flow in s and a minimization in $\mathbf{n}$ as a way to compute minimizers of (2.1) and (2.13). We begin with its description for the continuous system and verify that it has a monotone energy decreasing property. We then do the same for the discrete system.

4.1. Continuous case. We introduce the following subspace to enforce Dirichlet boundary conditions on open subsets Γ of $\partial\Omega$:

$$H^1_\Gamma(\Omega) = \{v \in H^1(\Omega) : v = 0 \text{ on } \Gamma\}. \tag{4.1}$$

4.1.1. First order variation. Consider the bulk energy $E[s, \mathbf{n}]$ where the pair $(s, \mathbf{n})$ is in the admissible class $\mathcal{A}$ defined in (2.3). We take a variation $z \in H^1_0(\Omega)$ of s and obtain $\delta_s E[s, \mathbf{n}; z] = \delta_s E_1[s, \mathbf{n}; z] + \delta_s E_2[s; z]$, the first variation of E in the direction z, where

$$\delta_s E_1[s, \mathbf{n}; z] = 2\int_\Omega (\nabla s \cdot \nabla z + |\nabla\mathbf{n}|^2 s z) \quad \text{and} \quad \delta_s E_2[s; z] = \int_\Omega \psi'(s) z.$$

Next, we introduce the space of tangential variations of $\mathbf{n}$:

$$V^{\perp}(\mathbf{n}) = \left\{ \mathbf{v} \in H^1(\Omega)^d : \mathbf{v} \cdot \mathbf{n} = 0 \text{ a.e. in } \Omega \right\}. \tag{4.2}$$

In order to satisfy the constraint $|\mathbf{n}| = 1$, we take a variation $\mathbf{v} \in V^{\perp}(\mathbf{n})$ of $\mathbf{n}$ and get

$$\delta_{\mathbf{n}} E[s, \mathbf{n}; \mathbf{v}] = \delta_{\mathbf{n}} E_1[s, \mathbf{n}; \mathbf{v}] = 2 \int_{\Omega} s^2 (\nabla \mathbf{n} \cdot \nabla \mathbf{v}).$$

Note that variations in $V^{\perp}(\mathbf{n})$ preserve the unit length constraint up to second order accuracy [45]: $|\mathbf{n} + t\mathbf{v}|^2 = 1 + t^2 |\mathbf{v}|^2$ and $|n + t\mathbf{v}| \geq 1$ for all $t \in \mathbb{R}$.

4.1.2. Quasi-gradient flow. We consider an L^2-gradient flow for E with respect to the scalar variable $s(t)$:

$$\int_{\Omega} \partial_t s z := -\delta_s E_1[s, \mathbf{n}; z] - \delta_s E_2[s; z] \quad \text{for all } z \in H^1_{\Gamma_s}(\Omega);$$

here, we enforce stationary Dirichlet boundary conditions for s on the set $\Gamma_s \subset \partial\Omega$, whence $z = 0$ on Γ_s. A simple but formal integration by parts yields

$$\int_{\Omega} \partial_t s z = -\int_{\Omega} \big(-2\Delta s + 2|\nabla \mathbf{n}|^2 s + \psi'(s) \big) z \qquad \text{for all } z \in H^1_{\Gamma_s}(\Omega),$$

where we use the implicit Neumann condition $\boldsymbol{\nu} \cdot \nabla s = 0$ on $\partial\Omega \setminus \Gamma_s$, $\boldsymbol{\nu}$ being the outer unit normal on $\partial\Omega$. Therefore, s satisfies the (nonlinear) parabolic PDE:

$$\partial_t s = 2\Delta s - 2|\nabla \mathbf{n}|^2 s - \psi'(s). \tag{4.3}$$

Given s, let $\mathbf{n}$ satisfy $|\mathbf{n}| = 1$ a.e. in Ω, a stationary Dirichlet boundary condition on the open set $\Gamma_{\mathbf{n}} \subset \partial\Omega$, and the following degenerate minimization problem:

$$E[s, \mathbf{n}] \leq E[s, \mathbf{m}] \quad \text{for all } |\mathbf{m}| = 1 \text{ a.e. } \Omega,$$

with the same boundary condition as $\mathbf{n}$. This implies

$$\delta_{\mathbf{n}} E[s, \mathbf{n}; \mathbf{v}] = 0 \quad \text{for all } \mathbf{v} \in V^{\perp}(\mathbf{n}) \cap H^1_{\Gamma_{\mathbf{n}}}(\Omega)^d. \tag{4.4}$$

4.1.3. Formal energy decreasing property. Differentiating the energy $E[s, \mathbf{n}]$ with respect to time, we obtain

$$\partial_t E[s, \mathbf{n}] = \delta_s E[s, \mathbf{n}; \partial_t s] + \delta_{\mathbf{n}} E[s, \mathbf{n}; \partial_t \mathbf{n}].$$

By virtue of (4.3) and (4.4), we deduce that

$$\partial_t E[s, \mathbf{n}] = -\delta_s E[s, \mathbf{n}; \partial_t s] = -\int_{\Omega} |\partial_t s|^2. \tag{4.5}$$

Hence, the bulk energy E is monotonically decreasing for our quasi-gradient flow.

4.2. Discrete case. Let $s_h^k \in \mathbb{S}_h(\Gamma_s, g_h)$ and $\mathbf{n}_h^k \in \mathbb{N}_h(\Gamma_{\mathbf{n}}, \mathbf{r}_h)$ denote finite element functions, where k indicates a "time-step" index (see Section 4.2.2 for the discrete gradient flow algorithm). To simplify notation, we use the following:

$$s_i^k := s_h^k(x_i), \quad \mathbf{n}_i^k := \mathbf{n}_h^k(x_i), \quad z_i := z_h(x_i), \quad \mathbf{v}_i := \mathbf{v}_h(x_i).$$

4.2.1. First order variation. First, we introduce the discrete version of (4.2):

$$V_h^{\perp}(\mathbf{n}_h) = \{\mathbf{v}_h \in \mathbb{U}_h : \mathbf{v}_h(x_i) \cdot \mathbf{n}_h(x_i) = 0 \text{ for all nodes } x_i \in \mathcal{N}_h\}. \tag{4.6}$$

Next, the first order variation of E_1^h in the direction $\mathbf{v}_h \in V_h^{\perp}(\mathbf{n}_h^k) \cap H^1_{\Gamma_{\mathbf{n}}}(\Omega)$ at the director variable $\mathbf{n}_h^k$ reads

$$\delta_{\mathbf{n}_h} E_1^h[s_h^k, \mathbf{n}_h^k; \mathbf{v}_h] = \sum_{i,j=1}^{N} k_{ij} \left(\frac{(s_i^k)^2 + (s_j^k)^2}{2} \right) (\delta_{ij}\mathbf{n}_h^k) \cdot (\delta_{ij}\mathbf{v}_h), \tag{4.7}$$

whereas the first order variation of E_1^h in the direction $z_h \in \mathbb{S}_h \cap H^1_{\Gamma_s}(\Omega)$ at the degree of orientation variable s_h^k consists of two terms

$$\delta_{s_h} E_1^h[s_h^k, \mathbf{n}_h^k; z_h] = \kappa \sum_{i,j=1}^{N} k_{ij} \left(\delta_{ij} s_h^k\right) (\delta_{ij} z_h) + \sum_{i,j=1}^{N} k_{ij} |\delta_{ij}\mathbf{n}_h^k|^2 \left(\frac{s_i^k z_i + s_j^k z_j}{2} \right). \tag{4.8}$$

To design an unconditionally stable scheme for the discrete gradient flow, we employ the convex splitting technique in [49, 41, 42]. We split the double well potential into a convex and concave part: let ψ_c and ψ_e be both convex for all $s \in (-1/2, 1)$ so that $\psi(s) = \psi_c(s) - \psi_e(s)$, and set

$$\delta_{s_h} E_2^h[s_h^{k+1}; z_h] := \int_\Omega \left[\psi_c'(s_h^{k+1}) - \psi_e'(s_h^k)\right] z_h dx. \tag{4.9}$$

Lemma 4.1 (convex-concave splitting). *For any s_h^k and s_h^{k+1} in $\mathbb{S}_h$, we have*

$$\int_\Omega \psi(s_h^{k+1}) dx - \int_\Omega \psi(s_h^k) dx \le \delta_{s_h} E_2^h[s_h^{k+1}; s_h^{k+1} - s_h^k].$$

Proof. A simple calculation, based on the mean-value theorem and the convex splitting $\psi = \psi_c - \psi_e$, yields

$$\int_\Omega \left(\psi(s_h^{k+1}) - \psi(s_h^k)\right) dx = \delta_{s_h} E_2^h[s_h^{k+1}; s_h^{k+1} - s_h^k] + T,$$

where

$$\begin{aligned} T = & \int_\Omega \int_0^1 \left[\psi_c'(s_h^k + \theta(s_h^{k+1} - s_h^k)) - \psi_c'(s_h^{k+1})\right](s_h^{k+1} - s_h^k) d\theta dx \\ & + \int_\Omega \int_0^1 \left[\psi_e'(s_h^k) - \psi_e'(s_h^k + \theta(s_h^{k+1} - s_h^k))\right](s_h^{k+1} - s_h^k) d\theta dx. \end{aligned}$$

The convexity of both ψ_c and ψ_e implies $T \le 0$, as desired. □

4.2.2. Discrete quasi-gradient flow algorithm. Our scheme for minimizing the discrete energy $E_h[s_h, \mathbf{n}_h]$ is an alternating direction method, which minimizes with respect to $\mathbf{n}_h$ and evolves s_h separately in the steepest descent direction during each iteration. Therefore, this algorithm is not a standard gradient flow but rather a quasi-gradient flow.

Algorithm: Given $(s_h^0, \mathbf{n}_h^0)$ in $\mathbb{S}_h(\Gamma_s, g) \times \mathbb{N}_h(\Gamma_{\mathbf{n}}, \mathbf{r})$, iterate Steps (a)-(c) for $k \geq 0$.

Step (a): Minimization. Find $\mathbf{t}_h^k \in V_h^{\perp}(\mathbf{n}_h^k) \cap H^1_{\Gamma_{\mathbf{n}}}(\Omega)$ such that $\mathbf{n}_h^k + \mathbf{t}_h^k$ minimizes the energy $E_1^h[s_h^k, \mathbf{n}_h^k + \mathbf{v}_h]$ for all $\mathbf{v}_h$ in $V_h^{\perp}(\mathbf{n}_h^k) \cap H^1_{\Gamma_{\mathbf{n}}}(\Omega)$, i.e. $\mathbf{t}_h^k$ satisfies

$$\delta_{\mathbf{n}_h} E_1^h[s_h^k, \mathbf{n}_h^k + \mathbf{t}_h^k; \mathbf{v}_h] = 0, \ \forall \mathbf{v}_h \in V_h^{\perp}(\mathbf{n}_h^k) \cap H^1_{\Gamma_{\mathbf{n}}}(\Omega).$$

Step (b): Projection. Normalize $\mathbf{n}_i^{k+1} := \frac{\mathbf{n}_i^k + \mathbf{t}_i^k}{|\mathbf{n}_i^k + \mathbf{t}_i^k|}$ at all nodes $x_i \in \mathcal{N}_h$.

Step (c): Gradient flow. Using $(s_h^k, \mathbf{n}_h^{k+1})$, find s_h^{k+1} in $\mathbb{S}_h(\Gamma_s, g)$ such that

$$\int_\Omega \frac{s_h^{k+1} - s_h^k}{\delta t} z_h = -\delta_{s_h} E_1^h[s_h^{k+1}, \mathbf{n}_h^{k+1}; z_h] - \delta_{s_h} E_2^h[s_h^{k+1}; z_h], \ \forall z_h \in \mathbb{S}_h \cap H^1_{\Gamma_s}(\Omega).$$

We impose Dirichlet boundary conditions for both s_h^k and $\mathbf{n}_h^k$. Note that the scheme has no restriction on the time step thanks to the implicit Euler method in Step (c).

4.3. Energy decreasing property. The quasi-gradient flow scheme in Section 4.2.2 has a monotone energy decreasing property, a discrete version of (4.5), provided the mesh $\mathcal{T}_h$ is weakly acute, namely it satisfies (2.6) [21, 43].

THEOREM 4.2 (energy decrease). *Let $\mathcal{T}_h$ satisfy* (2.6). *The iterate* $(s_h^{k+1}, \mathbf{n}_h^{k+1})$ *of the Algorithm (discrete quasi-gradient flow) of Section* (4.2.2) *exists and satisfies*

$$E^h[s_h^{k+1}, \mathbf{n}_h^{k+1}] \leq E^h[s_h^k, \mathbf{n}_h^k] - \frac{1}{\delta t} \int_\Omega (s_h^{k+1} - s_h^k)^2 dx.$$

Equality holds if and only if $(s_h^{k+1}, \mathbf{n}_h^{k+1}) = (s_h^k, \mathbf{n}_h^k)$ *(equilibrium state).*

Proof. The Steps (a) and (b) are monotone whereas Step (c) decreases the energy.

Step (a): Minimization. Since E_1^h is convex in $\mathbf{n}_h^k$ for fixed s_h^k, there exists a tangential variation $\mathbf{t}_h^k$ which minimizes $E_1^h[s_h^k, \mathbf{n}_h^k + \mathbf{v}_h^k]$ among all tangential variations $\mathbf{v}_h^k$. The fact that E_2^h is independent of the director field $\mathbf{n}_h^k$ implies

$$E^h[s_h^k, \mathbf{n}_h^k + \mathbf{t}_h^k] \leq E^h[s_h^k, \mathbf{n}_h^k].$$

Step (b): Projection. Since the mesh $\mathcal{T}_h$ is weakly acute, we claim that

$$\mathbf{n}_h^{k+1} = \frac{\mathbf{n}_h^k + \mathbf{t}_h^k}{|\mathbf{n}_h^k + \mathbf{t}_h^k|} \quad \Rightarrow \quad E_1^h\big[s_h^k, \mathbf{n}_h^{k+1}\big] \leq E_1^h\big[s_h^k, \mathbf{n}_h^k + \mathbf{t}_h^k\big].$$

We follow [1, 8]. Let $\mathbf{v}_h = \mathbf{n}_h^k + \mathbf{t}_h^k$, $\mathbf{w}_h = \frac{\mathbf{v}_h}{|\mathbf{v}_h|}$, and observe that $|\mathbf{v}_h| \geq 1$ and $\mathbf{w}_h$ is well-defined. By (2.11) (definition of discrete energy), we only need to show that

$$k_{ij} \frac{(s_i^k)^2 + (s_j^k)^2}{2} |\mathbf{w}_h(x_i) - \mathbf{w}_h(x_j)|^2 \leq k_{ij} \frac{(s_i^k)^2 + (s_j^k)^2}{2} |\mathbf{v}_h(x_i) - \mathbf{v}_h(x_j)|^2.$$

for all $x_i, x_j \in \mathcal{N}_h$. Because $k_{ij} \geq 0$ for $i \neq j$, this is equivalent to showing that $|\mathbf{w}_h(x_i) - \mathbf{w}_h(x_j)| \leq |\mathbf{v}_h(x_i) - \mathbf{v}_h(x_j)|$. This follows from the fact that the mapping $\mathbf{a} \mapsto \mathbf{a}/|\mathbf{a}|$ defined on $\{\mathbf{a} \in \mathbb{R}^d : |\mathbf{a}| \geq 1\}$ is Lipschitz continuous with constant 1. Note that equality above holds if and only if $\mathbf{n}_h^{k+1} = \mathbf{n}_h^k$ or equivalently $\mathbf{t}_h^k = \mathbf{0}$.

Step (c): Gradient flow. Since E_1^h is quadratic in terms of s_h^k, and

$$2 s_h^{k+1} \big(s_h^{k+1} - s_h^k\big) = \big(s_h^{k+1} - s_h^k\big)^2 + \big|s_h^{k+1}\big|^2 - \big|s_h^k\big|^2,$$

reordering terms gives

$$E_1^h[s_h^{k+1}, \mathbf{n}_h^{k+1}] - E_1^h[s_h^k, \mathbf{n}_h^{k+1}] = R_1 - E_1^h[s_h^{k+1} - s_h^k, \mathbf{n}_h^{k+1}] \leq R_1,$$

where

$$R_1 := \delta_{s_h} E_1^h[s_h^{k+1}, \mathbf{n}_h^{k+1}; s_h^{k+1} - s_h^k].$$

On the other hand, Lemma 4.1 implies

$$E_2^h[s_h^{k+1}] - E_2^h[s_h^k] = \int_\Omega \psi(s_h^{k+1})dx - \int_\Omega \psi(s_h^k)dx \leq R_2 := \delta_{s_h} E_2^h[s_h^{k+1}; s_h^{k+1} - s_h^k].$$

Combining both estimates and invoking Step (c) of the Algorithm yields

$$E^h[s_h^{k+1}, \mathbf{n}_h^{k+1}] - E^h[s_h^k, \mathbf{n}_h^{k+1}] \leq R_1 + R_2 = -\frac{1}{\delta t}\int_\Omega (s_h^{k+1} - s_h^k)^2 \leq 0,$$

which is the assertion. Note finally that equality occurs if and only if $s_h^{k+1} = s_h^k$ and $\mathbf{n}_h^{k+1} = \mathbf{n}_h^k$, which corresponds to an equilibrium state. This completes the proof. □

5. Numerical experiments. We present computational experiments to illustrate our method, which was implemented with the MATLAB/C++ finite element toolbox FELICITY [46]. For all 3-D simulations, we used the algebraic multi-grid solver (AGMG) [37, 35, 36, 38] to solve the linear systems in parts (a) and (c) of the quasi-gradient flow algorithm. In 2-D, we simply used the "backslash" command in MATLAB.

5.1. Tangential variations. Solving step (a) of the Algorithm requires a tangential basis for the test function and the solution. However, forming the matrix system is easily done by first ignoring the tangential variation constraint (i.e. arbitrary variations), followed by a simple modification of the matrix system.

Let $A\mathbf{t}_h^k = B$ represent the linear system in Step (a) and suppose $d = 3$. Multiplying by a discrete test function $\mathbf{v}_h$, we have

$$\mathbf{v}_h^T A\mathbf{t}_h^k = \mathbf{v}_h^T B, \quad \text{for all } \mathbf{v}_h \in \mathbb{R}^{dN}.$$

Next, using $\mathbf{n}_h^k$, find $\mathbf{r}_1$, $\mathbf{r}_2$ such that $\{\mathbf{n}_h^k, \mathbf{r}_1, \mathbf{r}_2\}$ forms an orthonormal basis of $\mathbb{R}^3$ at each node x_i, i.e. find an orthonormal basis of $V_h^\perp(\mathbf{n}_h^k)$. Next, expand $\mathbf{t}_h^k = \Phi_1\mathbf{r}_1 + \Phi_2\mathbf{r}_2$ and make a similar expansion for $\mathbf{v}_h$. After a simple rearrangement and partitioning of the linear system, one finds it decouples into two smaller systems: one for Φ_1 and one for Φ_2. After solving for Φ_1, Φ_2, define the nodal values of $\mathbf{t}_h^k$ by the formula $\mathbf{t}_h^k = \Phi_1\mathbf{r}_1 + \Phi_2\mathbf{r}_2$.

5.2. Point defect in 2-D. For the classic Frank energy $\int_\Omega |\nabla\mathbf{n}|^2$, a point defect in two dimensions has infinite energy [45]. This is not the case for the energy (2.1), because s can go to zero at the location of the point defect, so the term $\int_\Omega s^2|\nabla\mathbf{n}|^2$ will be finite.

We simulate the gradient flow evolution of a point defect moving to the center of the domain (Ω is the unit square). We set $\kappa = 2$ and take the double well potential to have the following splitting:

$$\begin{aligned}\psi(s) &= \psi_c(s) - \psi_e(s)\\ &= 63.0s^2 - (-16.0s^4 + 21.33333333333s^3 + 57.0s^2),\end{aligned}$$

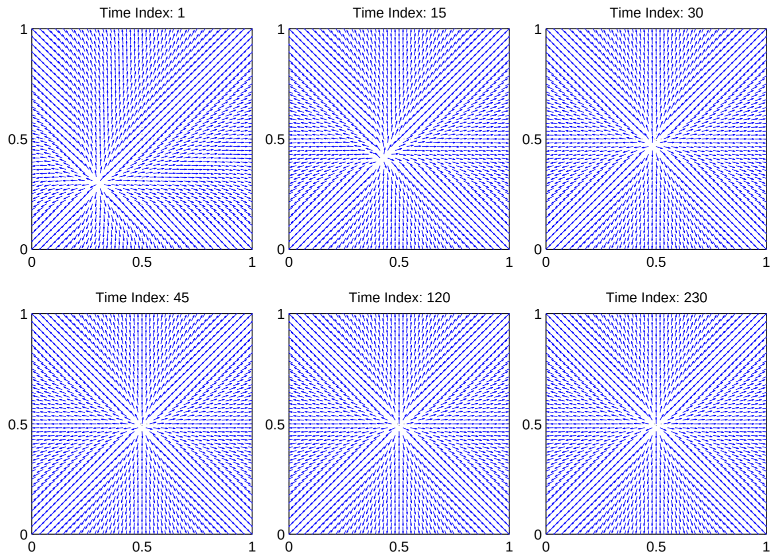

(a) Director field $\mathbf{n}$.

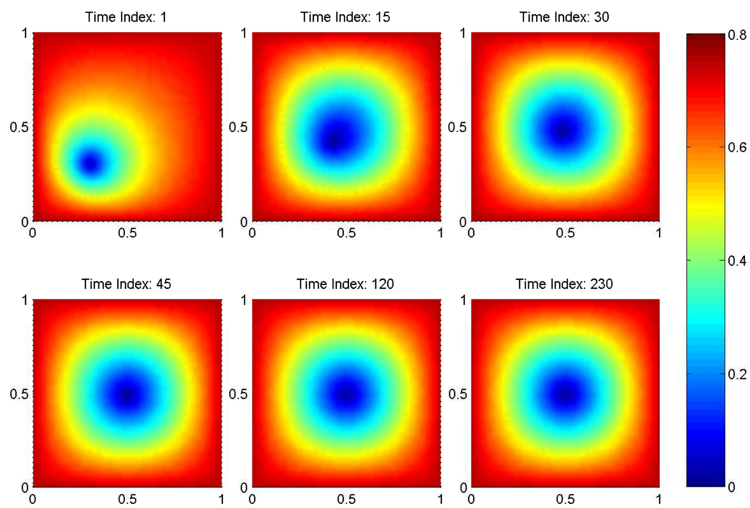

(b) Degree of orientation parameter s.

Fig. 5.1: Evolution of a point defect toward its equilibrium state (Section 5.2). Time step is $\delta t = 0.02$. The minimum value of s, at time index 230, is $2.0226 \cdot 10^{-2}$.

with a local minimum at $s = 0$ and global minimum at $s = s^* := 0.750025$ (see Section 2.1 for more information). The following Dirichlet boundary conditions on $\partial\Omega$ are imposed for s and $\mathbf{n}$:

$$s = s^*, \qquad \mathbf{n} = \frac{(x,y) - (0.5, 0.5)}{|(x,y) - (0.5, 0.5)|}. \tag{5.1}$$

Initial conditions on Ω for the gradient flow are: $s = s^*$ and a regularized point defect away from the center.

Figure 5.1 shows the evolution of the director field $\mathbf{n}$ and the scalar degree of orientation parameter s. One can see the regularizing effect that s has. We note that an L^2 gradient flow scheme, instead of the quasi (weighted) gradient flow we use, yields a much slower evolution to equilibrium.

5.3. Plane defect in 3-D. Next, we simulate the gradient flow evolution of the liquid crystal director field toward a *plane* defect on a cube domain ($\Omega = (0,1)^3$ is the unit cube). This is motivated by an exact solution found in [45, Sec. 6.4]. We set $\kappa = 0.2$ and *remove* the double well potential. The following Dirichlet boundary conditions on $\overline{\partial\Omega} \cap (\{z = 0\} \cup \{z = 1\})$ are imposed for $(s, \mathbf{n})$:

$$\begin{aligned} z = 0: \quad s &= s^*, \qquad \mathbf{n} = (1,0,0), \\ z = 1: \quad s &= s^*, \qquad \mathbf{n} = (0,1,0), \end{aligned} \tag{5.2}$$

and Neumann conditions are imposed on the remaining part of $\partial\Omega$, i.e. $\boldsymbol{\nu} \cdot \nabla s = 0$ and $\boldsymbol{\nu} \cdot \nabla \mathbf{n} = 0$. The exact solution $(s, \mathbf{n})$ (at equilibrium) only depends on z and is given by

$$\begin{aligned} &\mathbf{n}(z) = (1,0,0), \text{ for } z < 0.5, \quad \mathbf{n}(z) = (0,1,0), \text{ for } z > 0.5, \\ &s(z) = 0, \text{ at } z = 0.5, \text{ and } s(z) \text{ is linear for } z \in (0,0.5) \cup (0.5,1.0). \end{aligned} \tag{5.3}$$

Initial conditions on Ω for the gradient flow are: $s = s^*$ and a regularized point defect away from the center of the cube.

Figure 5.2 shows the evolution of the director field $\mathbf{n}$ toward the plane defect. Only a few slices are shown in Figure 5.2 because of the simple form of the equilibrium solution.

Figure 5.3 (left) shows the components of $\mathbf{n}$ evaluated along a one dimensional vertical slice. Clearly, the numerical solution approximates the exact solution well, except at the narrow transition region near $z = 0.5$. Furthermore, Figure 5.3 (right) shows the corresponding evolution of the degree of orientation parameter s (evaluated along the same one dimensional vertical slice). One can see the regularizing effect that s has, i.e. at equilibrium, $s \approx 0.008$ at the $z = 0.5$ plane (the defect plane of $\mathbf{n}$). Our numerical experiments suggest that $s|_{z=0.5} \to 0$ as the mesh size goes to zero.

5.4. Fluting effect and propeller defect. This example further investigates the effect of κ on the presence of defects. An exact solution of a line defect in a right circular cylinder is given in [45, Sec. 6.5]. They show that for κ sufficiently large (say $\kappa > 1$) the director field is smooth, but if κ is sufficiently small, then a line defect in $\mathbf{n}$ appears along the axis of the cylinder. Our numerical experiments confirm this.

To further illustrate this effect, we conducted a similar experiment for a unit cube domain $\Omega = (0,1)^3$. Again, for simplicity, we *remove* the double well potential. The following Dirichlet boundary conditions on the vertical sides of the cube $\overline{\partial\Omega} \cap (\{x = 0\} \cup \{x = 1\} \cup \{y = 0\} \cup \{y = 1\})$ are imposed for $(s, \mathbf{n})$:

$$s = s^*, \qquad \mathbf{n}(x,y,z) = \frac{(x,y) - (0.5,0.5)}{|(x,y) - (0.5,0.5)|}, \tag{5.4}$$

and Neumann conditions are imposed on the top and bottom parts of $\partial\Omega$, i.e. $\boldsymbol{\nu} \cdot \nabla s = 0$ and $\boldsymbol{\nu} \cdot \nabla \mathbf{n} = 0$. Figure 5.4 shows the equilibrium solution when $\kappa = 2$. The z-component of $\mathbf{n}$ is *not* zero, i.e. it points out of the plane of the horizontal slice that we plot. This is referred to as the "fluting effect" (or escape to the third dimension

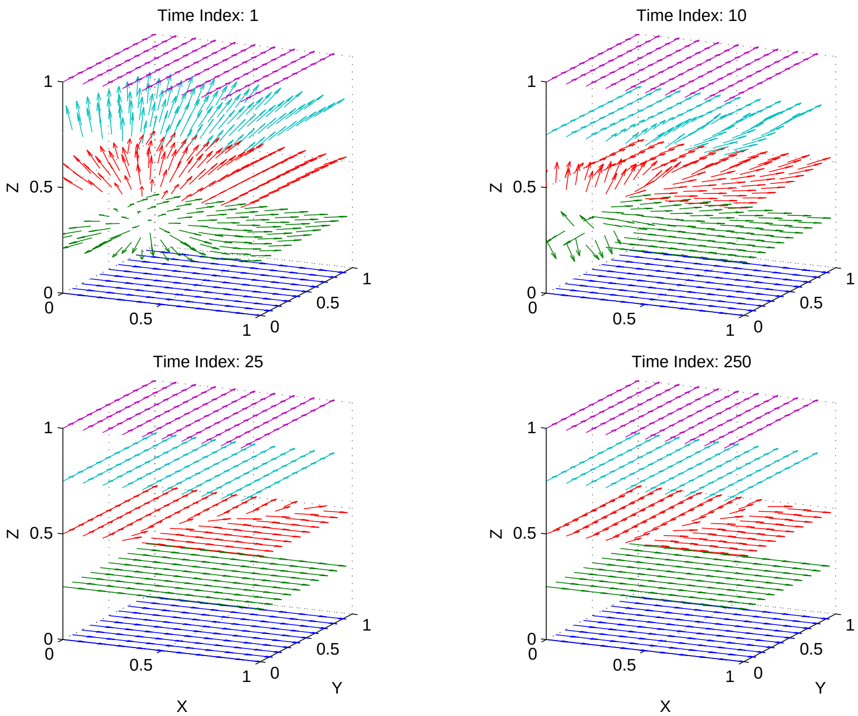

Fig. 5.2: Evolution toward an (equilibrium) plane defect (Section 5.3). The director field $\mathbf{n}$ is shown at five different horizontal slices. The time step used was $\delta t = 0.02$.

[45]). In this case, the degree of orientation parameter s is bounded well away from zero, so the director field is smooth (i.e. no defect).

Next, we choose $\kappa = 0.1$, and initialize our gradient flow scheme with $s = s^*$ and a regularized point defect away from the center of the cube for $\mathbf{n}$. Figure 5.5 shows the evolution of the director field $\mathbf{n}$ toward a "propeller" defect (two plane defects intersecting). Figure 5.6 shows $\mathbf{n}$ and s in their final equilibrium state at the $z = 0.5$ plane. Both $\mathbf{n}$ and s are nearly uniform with respect to the z variable. The regularizing effect of s is apparent, i.e. $s \approx 2 \times 10^{-5}$ near where $\mathbf{n}$ has a discontinuity. The 3-D shape of the defect resembles two planes intersecting near the $x = 0.5$, $y = 0.5$ vertical line, i.e. the defect looks like an "X" extruded in the z direction.

5.5. Floating plane defect. This example investigates the effect of the domain shape on the defect. The setup here is essentially the same as in Section 5.4, with $\kappa = 0.1$, except the domain is a rectangular box: $\Omega = (0, 1) \times (0, 0.7143) \times (0, 1)$. Figure 5.7 shows $\mathbf{n}$ and s in their final equilibrium state at the $z = 0.5$ plane. Both $\mathbf{n}$ and s are approximately uniform with respect to the z variable. Instead of the propeller defect, we get a "floating" plane defect aligned with the major axis of the box. Again, the regularizing effect of s is apparent, i.e. $s \approx 7 \times 10^{-5}$ near where $\mathbf{n}$ has a discontinuity.

6. Conclusion. We introduced and analyzed a robust finite element method for a degenerate energy functional that models nematic liquid crystals with variable degree of orientation. We also developed a gradient flow scheme for computing energy

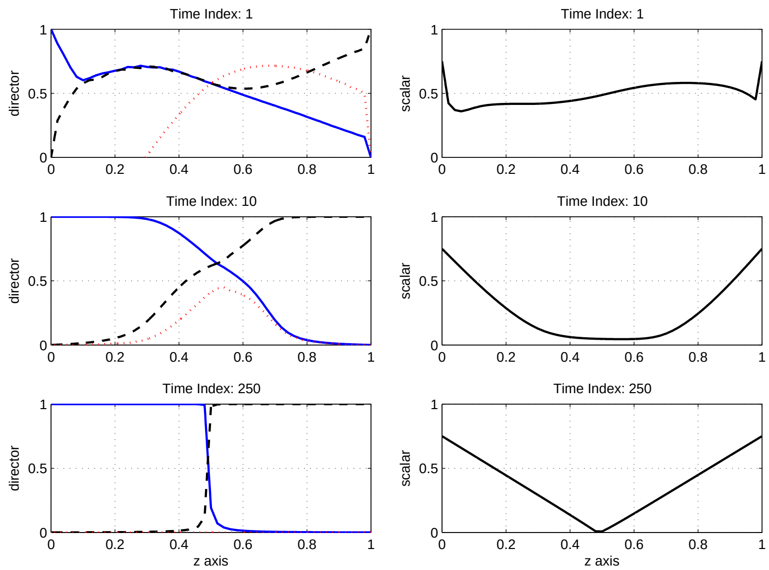

Fig. 5.3: Evolution toward an (equilibrium) plane defect (Section 5.3); time step is $\delta t = 0.02$. Left: plots of the three components of $\mathbf{n}$, evaluated along the vertical line $x = 0.5, y = 0.5$, are shown at three time indices (solid blue curve: $\mathbf{n} \cdot \mathbf{e}_1$, dashed black curve: $\mathbf{n} \cdot \mathbf{e}_2$, dotted red curve: $\mathbf{n} \cdot \mathbf{e}_3$). At equilibrium, $\mathbf{n}$ is nearly piecewise constant with a narrow transition region around $z = 0.5$. Right: plots of the degree-of-orientation s, corresponding to $\mathbf{n}$, are shown. The equilibrium solution is piecewise linear, with a kink at $z = 0.5$ where $s \approx 0.008$.

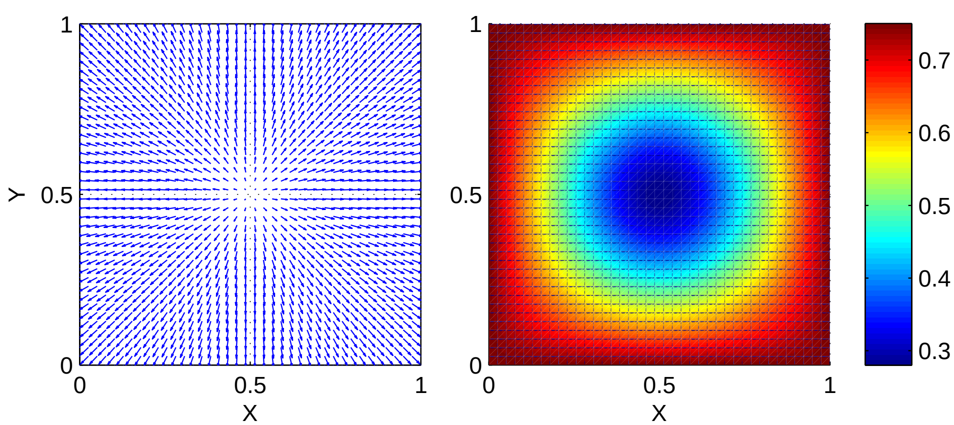

Fig. 5.4: Equilibrium state (Section 5.4) of $\mathbf{n}$ and s. One horizontal slice ($z = 0.5$) is plotted: $\mathbf{n}$ on the left, s on the right ($\mathbf{n}$ and s are approximately independent of z). The director field points out of the plane (i.e. $\mathbf{n} \cdot \mathbf{e}_3 \neq 0$) and $s > 0.278$, so there is no defect.

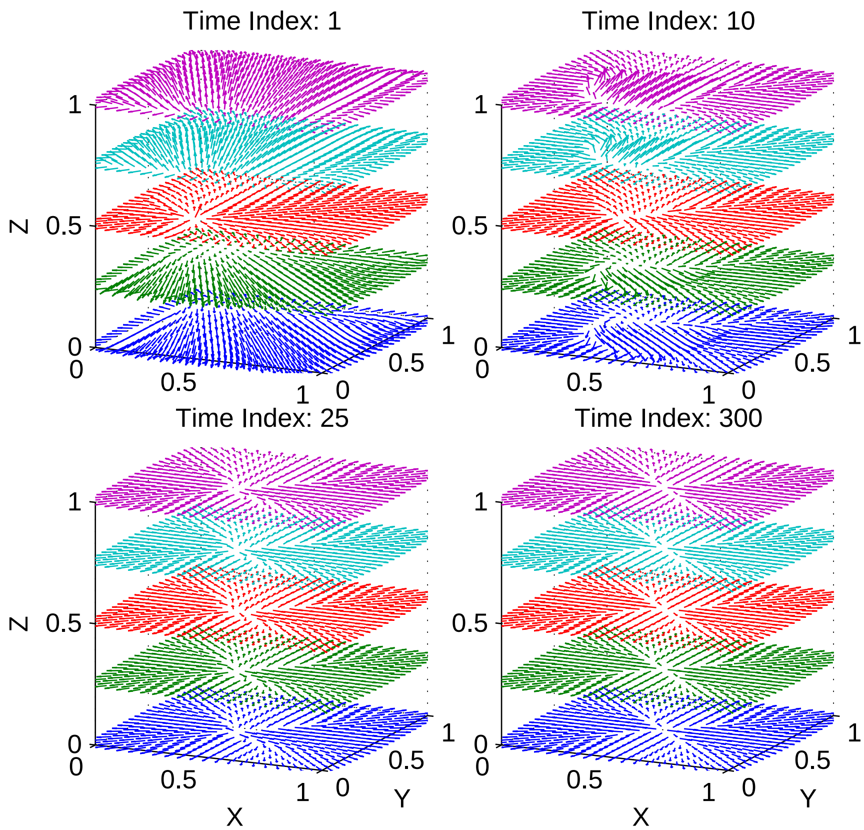

Fig. 5.5: Evolution toward an (equilibrium) "propeller" defect (Section 5.4). Director field $\mathbf{n}$ is shown at five different horizontal slices through the cube. The time step used was $\delta t = 0.02$.

minimizers, with a strict monotone energy decreasing property. The numerical experiments show a variety of defect structures that Ericksen's model exhibits. Some of the defect structures are high dimensional with surprising shapes (see Figure 5.6). An interesting extension of this work is to couple the effect of external fields (e.g. magnetic and electric fields) to the liquid crystal as way to drive and manipulate the defect structures.

Acknowledgements: Nochetto and Zhang acknowledge financial support by the National Science Foundation through the following grant DMS-1411808. Walker acknowledges financial support by the National Science Foundation through DMS-1418994. Zhang also acknowledges support through the Brin post-doctoral fellowship.

REFERENCES

[1] Francois Alouges, *A new algorithm for computing liquid crystal stable configurations: The harmonic mapping case*, SIAM Journal on Numerical Analysis, 34 (1997), pp. pp. 1708–1726.

[2] Luigi Ambrosio, *Existence of minimal energy configurations of nematic liquid crystals with variable degree of orientation*, Manuscripta Mathematica, 68 (1990), pp. 215–228.

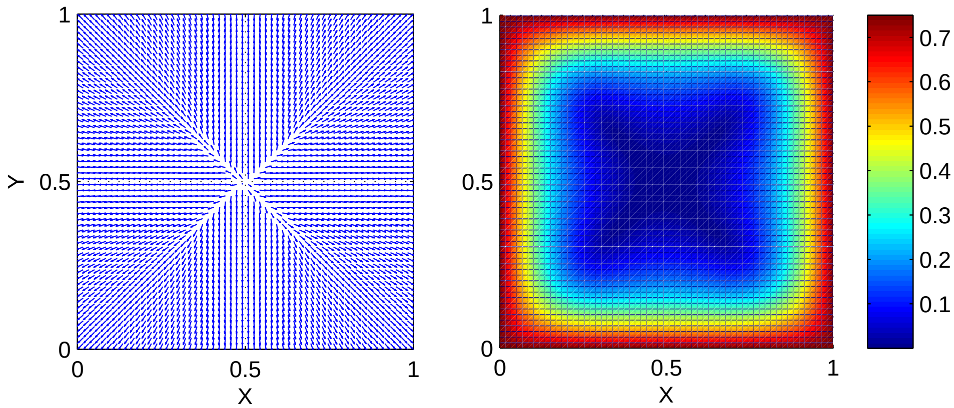

Fig. 5.6: Equilibrium state of a "propeller" defect (Section 5.4). One horizontal slice ($z = 0.5$) is plotted: $\mathbf{n}$ on the left, s on the right ($\mathbf{n}$ and s are nearly independent of z). The z-component of $\mathbf{n}$ is zero and $s \approx 2 \times 10^{-5}$ near the discontinuity in $\mathbf{n}$.

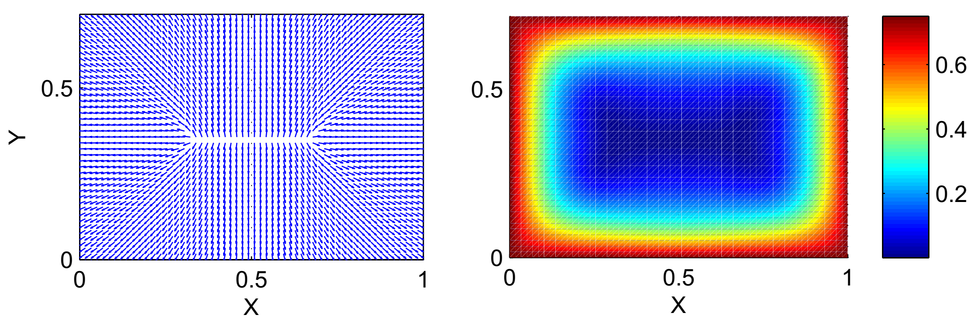

Fig. 5.7: Equilibrium state of a floating plane defect (Section 5.5). One horizontal slice ($z = 0.5$) is plotted: $\mathbf{n}$ on the left, s on the right ($\mathbf{n}$ and s are approximately independent of z). The z-component of $\mathbf{n}$ is zero and $s > 0$ with $s \approx 7 \times 10^{-5}$ near the discontinuity in $\mathbf{n}$.

[3] ———, *Regularity of solutions of a degenerate elliptic variational problem*, Manuscripta Mathematica, 68 (1990), pp. 309–326.

[4] Takeaki Araki and Hajime Tanaka, *Colloidal aggregation in a nematic liquid crystal: Topological arrest of particles by a single-stroke disclination line*, Phys. Rev. Lett., 97 (2006), p. 127801.

[5] S. Badia, F. M. Guillén-González, and J. V. Gutiérrez-Santacreu, *An overview on numerical analyses of nematic liquid crystal flows*, Archives of Computational Methods in Engineering, 18 (2011), pp. 285–313.

[6] John M. Ball and Arghir Zarnescu, *Orientability and energy minimization in liquid crystal models*, Archive for Rational Mechanics and Analysis, 202 (2011), pp. 493–535.

[7] John W. Barrett, Xiaobing Feng, and Andreas Prohl, *Convergence of a fully discrete finite element method for a degenerate parabolic system modelling nematic liquid crystals with variable degree of orientation*, ESAIM: Mathematical Modelling and Numerical Analysis, 40 (2006), pp. 175–199.

[8] Sören Bartels, *Stability and convergence of finite-element approximation schemes for harmonic maps*, SIAM Journal on Numerical Analysis, 43 (2006), pp. pp. 220–238.

[9] ———, *Numerical analysis of a finite element scheme for the approximation of harmonic maps*

into surfaces, Mathematics of Computation, 79 (2010), pp. 1263–1301.

[10] Sören Bartels, Georg Dolzmann, and Ricardo H. Nochetto, *A finite element scheme for the evolution of orientational order in fluid membranes*, ESAIM: Mathematical Modelling and Numerical Analysis, 44 (2010), pp. 1–31.

[11] ———, *Finite element methods for director fields on flexible surfaces*, Interfaces and Free Boundaries, 14 (2012), pp. 231 – 272.

[12] Patricia Bauman, M. Carme Calderer, Chun Liu, and Daniel Phillips, *The phase transition between chiral nematic and smectic a* liquid crystals*, Archive for Rational Mechanics and Analysis, 165 (2002), pp. 161–186.

[13] Brezis-H. Bethuel, F. and F. Hélein, *Ginzburg-Landau Vortices*, vol. 13 of Progress in Nonlinear Differential Equations and their Applications, Birkhäuser Boston Inc., Boston, MA, 1994.

[14] R. Byron Bird, Robert C. Armstrong, and Ole Hassager, *Dynamics of Polymeric Liquids - Volume 1: Fluid Mechanics*, vol. 1 of Wiley Interscience Publication, John Wiley and Sons, 2nd ed., 1987.

[15] L.M. Blinov, *Electro-optical and magneto-optical properties of liquid crystals*, Wiley, 1983.

[16] Andrea Braides, *Gamma-Convergence for Beginners*, vol. 22 of Oxford Lecture Series in Mathematics and Its Applications, Oxford Scholarship, 2002.

[17] ———, *Local minimization, variational evolution and* Γ*-convergence*, vol. 2094 of Lecture Notes in Mathematics, Springer, 2014.

[18] Jan H. Brandts, Sergey Korotov, and Michal Křížek, *The discrete maximum principle for linear simplicial finite element approximations of a reactiondiffusion problem*, Linear Algebra and its Applications, 429 (2008), pp. 2344 – 2357. Special Issue in honor of Richard S. Varga.

[19] Haïm Brezis, Jean-Michel Coron, and Elliott H. Lieb, *Harmonic maps with defects*, Communications in Mathematical Physics, 107 (1986), pp. 649–705.

[20] M. Calderer, D. Golovaty, F. Lin, and C. Liu, *Time evolution of nematic liquid crystals with variable degree of orientation*, SIAM Journal on Mathematical Analysis, 33 (2002), pp. 1033–1047.

[21] P.G. Ciarlet and P.-A. Raviart, *Maximum principle and uniform convergence for the finite element method*, Computer Methods in Applied Mechanics and Engineering, 2 (1973), pp. 17 – 31.

[22] Robert Cohen, San-Yih Lin, and Mitchell Luskin, *Relaxation and gradient methods for molecular orientation in liquid crystals*, Computer Physics Communications, 53 (1989), pp. 455 – 465.

[23] Gianni Dal Maso, *An introduction to* Γ*-convergence*, Progress in Nonlinear Differential Equations and their Applications, 8, Birkhäuser Boston, Inc., Boston, MA, 1993.

[24] P. G. de Gennes and J. Prost, *The Physics of Liquid Crystals*, vol. 83 of International Series of Monographs on Physics, Oxford Science Publication, Oxford, UK, 2nd ed., 1995.

[25] J.L. Ericksen, *Liquid crystals with variable degree of orientation*, Archive for Rational Mechanics and Analysis, 113 (1991), pp. 97–120.

[26] L. C. Evans, *Partial Differential Equations*, American Mathematical Society, Providence, Rhode Island, 1998.

[27] F. M. Guillén González and J. V. Gutiérrez-Santacreu, *A linear mixed finite element scheme for a nematic ericksenleslie liquid crystal model*, ESAIM: Mathematical Modelling and Numerical Analysis, 47 (2013), pp. 1433–1464.

[28] Robert Hardt, David Kinderlehrer, and Mitchell Luskin, *Remarks about the mathematical theory of liquid crystals*, in Calculus of Variations and Partial Differential Equations, Stefan Hildebrandt, David Kinderlehrer, and Mario Miranda, eds., vol. 1340 of Lecture Notes in Mathematics, Springer Berlin Heidelberg, 1988, pp. 123–138.

[29] Sergey Korotov, Michal Křížek, and Pekka Neittaanmäkia, *Weakened acute type condition for tetrahedral triangulations and the discrete maximum principle*, Math. Comput., 70 (2001), pp. 107–119.

[30] Ronald G. Larson, *The Structure and Rheology of Complex Fluids*, Oxford University Press, 1999.

[31] Fang-Hua Lin, *Nonlinear theory of defects in nematic liquid crystals; phase transition and flow phenomena*, Communications on Pure and Applied Mathematics, 42 (1989), pp. 789–814.

[32] Fang Hua Lin, *On nematic liquid crystals with variable degree of orientation*, Communications on Pure and Applied Mathematics, 44 (1991), pp. 453–468.

[33] San-Yih Lin and Mitchell Luskin, *Relaxation methods for liquid crystal problems*, SIAM Journal on Numerical Analysis, 26 (1989), pp. 1310–1324.

[34] C. Liu and N. Walkington, *Approximation of liquid crystal flows*, SIAM Journal on Numerical

Analysis, 37 (2000), pp. 725–741.
[35] Artem Napov and Yvan Notay, *Algebraic analysis of aggregation-based multigrid*, Numerical Linear Algebra with Applications, 18 (2011), pp. 539–564.
[36] ———, *An algebraic multigrid method with guaranteed convergence rate*, SIAM Journal on Scientific Computing, 34 (2012), pp. A1079–A1109.
[37] Yvan Notay, *An aggregation-based algebraic multigrid method*, Electronic Transactions On Numerical Analysis, 37 (2010), pp. 123–146.
[38] ———, *Aggregation-based algebraic multigrid for convection-diffusion equations*, SIAM Journal on Scientific Computing, 34 (2012), pp. A2288–A2316.
[39] R. G. Owens and Timothy N. Phillips, *Computational Rheology*, World Scientific Publishing Company, 2002.
[40] Richard Schoen and Karen Uhlenbeck, *A regularity theory for harmonic maps*, Journal of Differential Geometry, 17 (1982), pp. 307–335.
[41] J. Shen and X. Yang, *Numerical approximations of Allen-Cahn and Cahn-Hilliard equations*, Discrete Contin. Dyn. Syst., 28 (2010), pp. 1669 – 1691.
[42] J. Shen and X. Yang, *A phase-field model and its numerical approximation for two-phase incompressible flows with different densities and viscosities*, SIAM Journal of Scientific Computing, 32 (2010), p. 11591179.
[43] Gilbert Strang and George Fix, *An Analysis of the Finite Element Method*, Wellesley-Cambridge, 2nd ed., May 2008.
[44] K. Tojo, A. Furukawa, T. Araki, and A. Onuki, *Defect structures in nematic liquid crystals around charged particles*, The European Physical Journal E, 30 (2009), pp. 55–64.
[45] E. G. Virga, *Variational Theories for Liquid Crystals*, vol. 8, Chapman and Hall, London, 1st ed., 1994.
[46] Shawn W. Walker, *FELICITY: Finite ELement Implementation and Computational Interface Tool for You*. http://www.mathworks.com/matlabcentral/fileexchange/31141-felicity.
[47] Noel J. Walkington, *Numerical approximation of nematic liquid crystal flows governed by the ericksen-leslie equations*, ESAIM: Mathematical Modelling and Numerical Analysis, 45 (2011), pp. 523–540.
[48] Richard L. Wheeden and Antoni Zygmund, *Measure and Integral: An Introduction to Real Analysis*, Marcel-Dekker, 1977.
[49] S. M. Wise, C. Wang, and J. S. Lowengrub, *An energy-stable and convergent finite-difference scheme for the phase field crystal equation*, SIAM J. Numer. Anal., 47 (2009), pp. 2269–2288.
[50] Xiaofeng Yang, M. Gregory Forest, Huiyuan Li, Chun Liu, Jie Shen, Qi Wang, and Falai Chen, *Modeling and simulations of drop pinch-off from liquid crystal filaments and the leaky liquid crystal faucet immersed in viscous fluids*, Journal of Computational Physics, 236 (2013), pp. 1 – 14.
[51] Xiaofeng Yang, M. Gregory Forest, Chun Liu, and Jie Shen, *Shear cell rupture of nematic liquid crystal droplets in viscous fluids*, Journal of Non-Newtonian Fluid Mechanics, 166 (2011), pp. 487 – 499.